TECHNISCHE UNIVERSITÄT WIEN
Vienna | Austria

DIPLOMARBEIT

Evaluation of Five Single-Sided Natural Ventilation Calculation Methods

unter der Leitung von

Univ.-Prof. Dipl.-Ing. Dr. Tech. Ardeshir Mahdavi

E 259-3 Abteilung für Bauphysik und Bauökologie

Institut für Architekturwissenschaften

eingereicht an der

Technischen Universität Wien

Fakultät für Architektur und Raumplanung

von

Alexandra Balmuș

1426347

Wien, November 2017 Unterschrift

KURZFASSUNG

Die natürliche Lüftung ist ein häufig verwendetes Prinzip und eine effiziente Strategie wenn es um den Entwurf von der Gebäuden mit einem geringeren Verbrauch and Kühlenergie und einer verbesserten Raumluftqualität geht. In der Entwurfsphase von der Gebäuden müssen Informationen über die Menge an der Frischluft vorliegen, die durch die Öffnungen in der Gebäudehülle kommt. In den letzten Jahren wurden daher viele natürliche Lüftungsmodelle zur Vorhersage der Luftwechselrate entwickelt: analytische / empirische Modelle, Netzwerkmodelle und Verfahren der numerischen Strömungsmechanik (CFD). Obwohl die letzten beiden Prinzipien prinzipiell zuverlässigere Vorhersagen der natürlichen Belüftung liefern können, in einer frühen Bauphase können die analytische Modelle eine schnelle und einfache Abschätzung der Luftwechselraten ermöglichen, ohne die Notwendigkeit von der umfangreichen Eingabeinformationen.

In der vorliegenden Arbeit werden die durch fünf einseitige natürliche Lüftungsberechnungsverfahren geschätzten Luftwechselraten durch vollmaßstäbliche Messungen in einem Universitätsgebäude in Wien bewertet. Die Messungen werden mit der Tracergas-Technik mit SF6 als Tracergas und unter Berücksichtigung verschiedener Szenarien von Fensteröffnungen durchgeführt. Anschließend werden die gemessenen Luftwechselraten mit denen aus den Lüftungsberechnungsverfahren verglichen, um die Vorhersagekraft der Modelle zu untersuchen. Diese Validierungsstudie ermöglicht es auch, die Quellen der Diskrepanz zwischen den gemessenen und geschätzten Luftwechselraten in verschiedenen Einstellungen hinsichtlich Fensterzuständen und äußeren Randbedingungen zu untersuchen.

Die Ergebnisse der Studie zeigen, dass zusätzlich zu der Öffnungsfläche, der Windgeschwindigkeit und der Temperaturdifferenz auch die Windrichtung einen signifikanten Einfluss auf die Luftwechselraten hat, die nicht bei allen Modellen erfassen würde. Darüber hinaus, im Fall der Modelle die die Öffnungsfläche berücksichtigen, sind die Vorhersagen hauptsächlich für kleinere Öffnungen genauer. Im Allgemeinen, kann argumentiert werden, dass drei der untersuchten Modelle Schätzungen die gut mit den Messungen übereinstimmen liefern.

ABSTRACT

Natural ventilation is a frequently used principle and an efficient strategy when it comes to designing buildings with a lower cooling energy demand and improved indoor air quality. In the design phase of buildings, it is necessary to have information about the quantity of fresh air coming through the openings in the buildings envelope. As a result, many natural ventilation models for prediction of air change rate have been developed in the past years: analytical/empirical models, network models and Computational Fluid Dynamics (CFD) techniques. Although the last two can in principle offer more reliable predictions of natural ventilation, in an early phase of building design, analytical models can offer a quick and simple estimation of the air change rates without requiring extensive input information.

In the present thesis the air change rates estimated by five single-sided natural ventilation calculation methods are evaluated through full-scale measurements in a university building in Vienna, Austria. The measurements are made using the tracer gas technique with SF_6 as tracer gas and considering different scenarios of window openings. Subsequently, the measured air change rates are compared with those obtained from the estimation methods in order to examine the models' predictive performance. This validation study also makes it possible to investigate the sources of discrepancy between the measured and estimated air change rates in different settings with regard to window states and outside boundary conditions.

The results of the study shows that besides opening area, wind velocity and temperature difference, wind direction also has a significant effect on the air change rates, which is not captured in all models. Besides, in case of the models which consider opening area, the predictions are mainly more accurate for smaller openings. In general, it can be argued that three of the studied models provide estimations with good agreement with the measurements.

Keywords

Natural ventilation, Single-sided ventilation, Air change rate, Calculation method, Tracer gas measurements

ACKNOWLEDGEMENTS

The work on this Master's Thesis would not have been done without the help and support of family, friends and professors and assistants of the Department of Building Physics and Building Technologies at Vienna University of Technology.

My gratitude goes to my supervisor Univ.-Prof. DI Dr. Ardeshir Mahdavi for assistance, guidance and great help in making this thesis possible. I would also like to thank Dr. Matthias Schuss and Dr. Farhang Tahmasebi for their professional collaboration, guidance and advice during this research.

I would like to express my acknowledgements to Dr. Markus Treiber, DI Jörg Babenz and M. Sc. Moritz-Andreas Decker from the company Drees & Sommer Advanced Building Technologies in Munich for their support and advice during my research.

Moreover, I would like to thank my family for the moral support and encouragement during my studies.

Finally, but not least, my special thanks go to my dear friend Julian for endless support, patience and faith in me.

CONTENTS

1 Introduction 1

1.1 Overview 1

1.2 Motivation 2

1.3 Background 2

1.3.1 Introduction to Natural Ventilation 2

1.3.2 Dependency of air change rates on weather conditions and window opening 5

1.3.3 Design phases and prediction methods of natural ventilation 5

1.3.4 Analytical and empirical methods of calculation for natural ventilation 7

1.3.5 Measurements of air change rates with tracer gas 16

1.4 Hypothesis 18

2 Method 19

2.1 Overview 19

2.2 The Selected Single-Sided Calculation Methods 19

2.3 Tracer Gas Measurements 23

2.3.1 Description of Measurements 23

2.3.2 The test room 24

2.3.3 External parameters 26

2.3.4 Internal parameters 27

2.3.5 Measurements during a test session 28

2.4 Data processing and calculations 29

3 Results and discussion 30

3.1 Measured air change rates 30

3.2 Calculated air change rates 33

3.2.1 Hansen's method (VDI 2078) 33

3.2.2 De Gids and Phaff's method (EN 15242) 33

3.2.3 DS method 34

3.2.4 ASHRAE HoF method 35

3.2.5 Warren's method 38
3.3 Comparative analysis of the models' predictive performance 38
4 Conclusion 46
5 Index 48
5.1 List of Figures 48
5.2 List of Tables 49
5.3 List of Equations 50
6 Literature 53
7 Appendix 57
A. Technical specification of WSBPI (Thies 2007) 57
B. Technical specifications Innova Gasmonitor 1312 58

1 INTRODUCTION

1.1 Overview

Natural ventilation is one of the most efficient design strategies when it comes to improving indoor air quality and reducing the cooling energy consumption of a building. Moreover, providing constant fresh air supply into a space can assure a comfortable and healthy indoor climate for its occupants. Different studies (Seppänen et al. 1999; Seppänen and Fisk 2004, Wargocki et al., 2002) highlight the importance of indoor air quality when it comes to the health of the residents. Furthermore, as Seppänen and Fisk (2004) present in their work, the natural ventilated buildings are linked with less Sick Building Syndrome symptoms as the ones with a mechanical ventilation system. In order to reach these goals, a minimum air change is required depending on the properties of each building (type, environmental systems, activity of occupants, etc.). Consequently, it is necessary, to have information about the quantity of fresh air coming through the openings in the buildings envelope already from the conceptual design phase. The air change rate is dependent of the driving forces which lead to natural ventilation in buildings: wind and thermal buoyancy. This process occurs through openings in the buildings envelope or different passive techniques, or it can just be the simple action of opening the window to let fresh air inside. Thus, the air change rate can be affected by the buildings' envelope, meteorological conditions, indoor environment and the occupants' behavior (Laussmann and Helm 2011). Many calculations methods for the prediction of air change rate through window ventilation, which take into consideration different influencing aspects, have been developed in the past years. Although cross-ventilation is more effective than single-sided ventilation due to its capability to create higher air change rates, its use is limited because of building regulations, unfavorable building shapes or interior layouts. Moreover, given that many of the buildings, commercial or residential, are usually planned having rooms with one-sided windows, it makes sense to specially investigate the case of single-sided natural ventilation.

Specifically, the focus of this study is to explore the predictability of the air change rates via existing methods for estimation of natural ventilation. This model validation study will be based on the data obtained from real-scale measurements in a university building in Vienna, Austria.

This research work is structured in terms of four chapters. Chapter 1 will present general notions of natural ventilation and a research on existing calculation methods

for single-sided natural ventilation. Chapter 2 describes the methodology, details about the case study, measurements, data collection and implementation. Chapter 3 presents the results and discussion and chapter 4 is dedicated to the conclusion of this study.

1.2 Motivation

One of the main issues in the design phases of buildings is to make sure a constant fresh air supply is provided into a space in order to assure a comfortable and healthy indoor climate for its occupants. In a design phase, simulations of buildings are made in order to obtain predictions of their performance. Natural ventilation is a complex phenomenon and as a design strategy it requires a lot of knowledge and attention to fulfil the desirable results in terms of ventilation rates. CFD (Computational fluid dynamics) simulations can offers good predictions of natural ventilation. However, performing CFD simulations is complex and also costly. Therefore this method is being used in the final design phase of a building. Analytical models of natural ventilation could offer simpler calculation methods for determining the amount of air entering a space, in particular for simple and single-zone geometries. Thereby, the purpose of this research is to analyze the performance of different estimation methods for single-sided natural ventilation and to compare their prediction capabilities. The verification and validation of the methods is performed through full-scale measurements in an office room at TU Wien (Vienna, Austria). Consequently, the results could show which models can provide reliable estimations of air change rates in buildings.

Thereby, the purpose of this research is to analyze the performance of five single-sided natural ventilation models. Specifically the study conducts a verification and validation of the models through full-scale measurements in a university building in Vienna, Austria.

1.3 Background

1.3.1 Introduction to Natural Ventilation

Natural ventilation is an effective design strategy which has the ability to improve the indoor air quality by replacing the indoor air with fresh outside air, improve thermal comfort by lowering the room temperatures when the outdoor air temperature is cooler, assure air flow to cool down the building structure, therefore reducing the

cooling energy consumption of a building and also support the occupants physiological cooling processes (Ghiabaklou 2010).

Providing fresh air into a space is a fundamental requirement for assuring indoor air quality, thus a healthy environment for a buildings occupants. Numerous papers investigating the differences between natural and mechanical ventilation have been written. Seppänen and Fisk (2004) conclude in their research that there are less Sick Building Syndrome symptoms in natural ventilated buildings as in the ones with a mechanical ventilation system. Hellwig et al. (2006) conducted a study in 14 German office buildings with the purpose to identify parameters that influence the perception of thermal comfort of the occupants. Six of the buildings were naturally ventilated buildings and the rest were equipped with mechanical ventilation. The results of the interviews revealed that the office workers in the naturally ventilated buildings were considerably more satisfied with their thermal comfort than the office workers in the buildings with mechanical ventilation system.

However, the effectiveness of natural ventilation as a design strategy highly depends on the climatic conditions as it is not considered practical in hot and humid climates or in cold climates (ASHRAE 2009). Therefore, it is important to integrate the natural ventilation concept already from the early design phases of a building. Defining the location, orientation, shape of the building, the ventilation principle and the size and control of the ventilation openings in good agreement with the natural driving forces can result in a good distribution of air flow through the building.

Natural ventilation is caused by temperature differences and wind pressure differences at the openings of a buildings envelope. It can occur by infiltration of outside air through unintentional openings in the structure or/and by the simple action of opening windows, doors and letting outside air to flow in and out of a space.

There are three types of ventilation principles that can be used in a building: single-sided ventilation, cross-ventilation and stack ventilation (Figure 1).

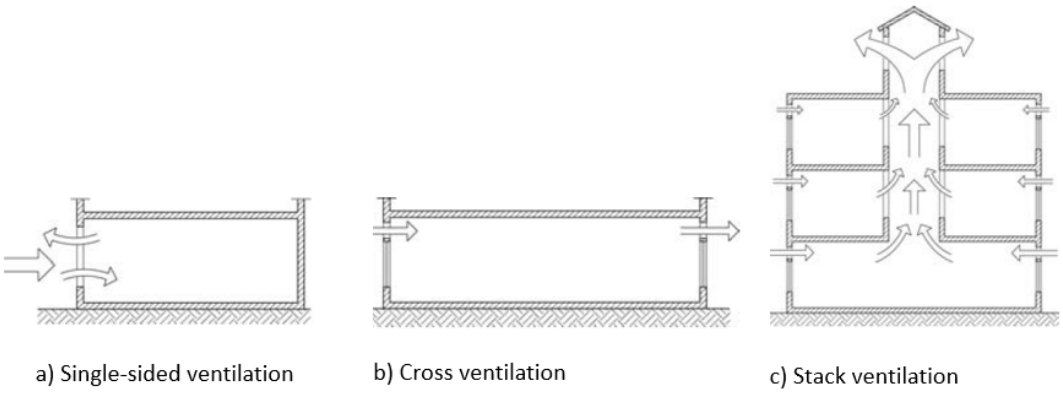

Figure 1 Natural ventilation principles: a) single-sided ventilation, b) cross ventilation and c) stack ventilation (source: Heiselberg 2006a)

Single-sided ventilation is the situation when the opening in the buildings envelope is only on one side of the room. The temperature differences are the main driving force in winter and wind pressure differences in summer. The ventilation rates generated in this case are lower than in the other cases because the air does not flow that far into the space. However, considering the design of another opening on the same side at a lower level increases the ventilation rate in the space (Heiselberg 2006a). Of great importance in the single-sided ventilation is also the size of the turbulent eddies at the openings and the pulsations in the flow (Larsen 2006).

In cross ventilation the openings are on two sides of the room, the ventilation occurring because of the wind pressure differences between the two openings. Although higher ventilation rates can be generated, it is difficult to control and to design as the main issue would the building form and its capacity to offer substantial differences in the wind pressure coefficient between the two openings. Another issue is the layout of the building and the interior partitions that can block the air flow.

The third principle, stack ventilation, is driven by thermal buoyancy and it occurs when the openings are at a low and high level in the building. This principle can offer high to moderate air ventilation rates, but it does need a lot of attention in design, as the position and the form of the stack outlet and the size of the inlets are of great importance (Heiselberg 2006a).

All three principle have an effect on the architecture of the building, specifically on its shape and its plan layout. Single-sided ventilation and cross ventilation are effective in linear buildings with narrow depths and stack ventilation involves the design of different ventilation elements like chimneys, atriums or wind towers.

1.3.2 Dependency of air change rates on weather conditions and window opening

Nowadays, numerous buildings are designed with a thick layer of insulation and airtight openings in the outside walls in order to minimize the leakage and improve the thermal performance. This leads to the necessity of providing fresh air into the space in order to offer a healthy and comfortable environment for the occupants. Planning natural ventilation in the design of a building with ventilative or “free” cooling is highly dependent on the climatic conditions. Natural ventilation occurs by the infiltration of outside air through leakage paths in a building’s envelope, by intentional openings that let outside air inside the building or/and by the simple action of opening windows and doors. Thus, natural ventilation is not only dependent on the building design, but also on the difficultly predictable weather conditions and occupant behavior. Therefore, especially from the view of HVAC engineers, natural ventilation poses a challenge for a robust building design.

Numerous studies address the effect of opening windows on air change rates. The study conducted by Howard-Reed et al. (2002) on two houses shows that, in relation with outdoor and indoor environment (temperature differences and wind effects), opening windows have a great effect on measured air change. The similar aspect was suggested by Wilson et al. (1996) when the results of a survey held in a residential area in southern California described the possible variation in air change rates due to operation of windows by occupants. Kvisgaard and Collet (1990) estimated that opening of windows and doors by the occupants in 17 Denmark homes caused 63 % of the total air change rate. This tendency of increased air change rates due to opening of the windows (i.e. occupant behavior) was observed also in other studies: Dick and Thomas 1951; Iwashita and Akasaka 1997; Roulet and Scartezzini 1987; Traynor et al. 1988.

Heiselberg (2006a) states that in tight energy efficient houses infiltration associated air change rates can have values of 0.1 to 0.2 h^{-1}, whereas in leaky houses the values can reach between 2 and 3 air change rates per hour. He also affirms that it is also possible to obtain values between 15 – 20 air change rates per hour by natural means with windows wide open during summer and even larger values if there are more window openings available with a strategic placement in the space.

1.3.3 Design phases and prediction methods of natural ventilation

Natural ventilation should be designed together with the building from the start of the design process as its effectiveness is highly dependent on numerous input

parameters like outdoor conditions, orientation, number and size of openings in a building's façade, layout and components of the building.

As Heiselberg (2006a) presents in his work, the design phases for implementing natural ventilation are as follows: conceptual design phase, basic design phase, detailed design phase and design evaluation phase.

In the conceptual design phase the input data of the building (form, location, orientation) are not well established. First predictions of air change rates are made in order to estimate window areas. In this phase the natural ventilation principle is chosen together with an additional mechanical system if necessary. In the basic design phase the necessary air flow rates, the expected indoor temperature levels and thermal loads are calculated and the ventilation system layout is also designed. During the detailed design phase the thermal loads are evaluated and the design of the building is optimized. In the last design phase (design evaluation phase), detailed predictions of indoor air quality and thermal comfort are made to see if the design satisfies the desired objectives.

A few prediction methods of natural ventilation have been developed through the past years. These methods are helpful because they can offer predictions of the air flow in a building for different phases of the design process: analytical and empirical/experimental methods, network methods and Computational Fluid Dynamics (CFD) methods.

The analytical and empirical methods offer a quick estimation of the air flow rate making them extremely useful in the conceptual and basic design phase, where the input data of the building is not well established yet. However, these models have been developed from theory and from experimental data and are based on assumptions and general correlations which may not offer accurate results when compared to measured data.

An improved prediction as required in the detailed design phase of the natural ventilation can be made by using network methods which take also the thermal dynamics of the building into considerations by using tools like TRNSYS, EnergyPlus and ESP-r and multizone air flow analysis tools like COMIS and CONTAM.

In the last phase of a building's design, where the input data and technical system is well known, using CFD analysis methods makes sense. Although these methods are costly and time consuming, they are able to offer precise predictions on the performance of the building in terms of ventilation system, indoor air quality, thermal comfort and energy consumption.

Zhai et al. reveal in their paper (Zhai et al. 2015) that the analytical models are appropriate for simple and single-zone geometries, while the network airflow models like COMIS, CONTAM and ESP-r are suitable for multi-zone structures and can be used to model different natural ventilation situation with an exception of the single-sided wind-driven case where the prediction of airflows are proved to be less accurate. From the literature review made in the above mentioned paper it is concluded that the existing network models have similar performances. It is also mentioned, that although CFD offers a good performance of the natural ventilation models it is not always the right solution because of its complexity and high costs.

Larsen et al. (2016) present in their paper a guidance for selecting the right calculation methods according to the design stages as shown in Table 1. At an early phase of the design process a simple and quick method for predicting the airflows makes sense, whereas at an advanced phase when most of the parameters are fixed (orientation of the building, dimension of openings in the building's façade, layout of interior space) a more complex calculation method could be realized. The purpose of the calculation is also important, considering that assuring a ventilative cooling and thermal comfort during summer time by means of natural ventilation is more difficult as assuring a proper indoor air quality in terms of fresh air entering a space through the façade's openings.

Table 1 Guidance for design stages for single-sided natural ventilation (source: Larsen et al. 2016)

	Conceptual design phase	Detailed design phase
Aim	Estimations of needed window areas based on : - Air flow rates - Cooling demands	Documentation of sufficient window areas based on: - Needed air flow rates - Cooling demands Documentation on thermal comfort and atmospheric comfort
Tools/Calculations	Simple and fast methods for estimations	Detailed calculations with detailed input, eg. CFD, airflow network
Target group	Architects, engineers, regulators	Engineers

1.3.4 Analytical and empirical methods of calculation for natural ventilation

When comparing cross-ventilation and single-sided ventilation it is already known that cross-ventilation has a better performance than single-sided ventilation since it is capable of providing larger air exchange rates. Still, design strategies for cross-

ventilation are usually limited because of strict building regulations, unfavorable layouts and building shapes. For this reason, it makes sense to investigate and focus on single-sided ventilation. However, the calculation of airflows in the case of single-sided ventilation seems to be more complicated as in the case of cross-ventilation because of the fluctuations in the airflow (Larsen 2006).

Since the driving forces which lead to natural ventilation in buildings are thermal buoyancy and wind, calculation methods which considers only one of the components as well as methods which considers a combination of both components have been researched in the past.

Airflows driven by thermal buoyancy

Single-sided ventilation driven by thermal buoyancy in one opening has a bidirectional flow which implies that the pressures are equal at the height of the neutral plane of the opening and the direction of the velocity changes at the level of the neutral pane as illustrated in Figure 2 (Heiselberg 2006b).

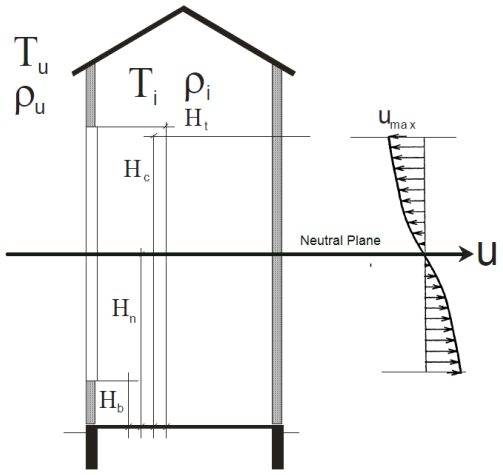

Figure 2 Velocity profile of the airflow for a single-sided large opening in the case of ventilation driven by thermal buoyancy (source: Heiselberg 2006)

P.R. Warren developed a simple design method (Warren et al. 1985) which calculates volume flow rate in the case of airflows caused by thermal buoyancy in a single opening as seen in Equation 1.

$$Q_s = \frac{1}{3} * A * C_d * \sqrt{\frac{\Delta T * H * g}{T_{ave}}} \quad (1)$$

Where Q_v is the volume flow rate [m^3/s], A is the area of the opening [m^2], C_d, the discharge coefficient [-], takes into consideration the shape of the opening and is usually taken as 0.6, ΔT is the temperature difference between inside and outside air temperature [K], H is the clear height of the opening [m], g is the gravitational acceleration [m/s^2] and T_{ave} is the average temperature between outdoor and indoor [K].

Another calculation method is the one presented in VDI 2078 Standard “Calculation of thermal loads and room temperatures” (2015). Annex A3 of the mentioned standard offers an “Approximation Formulae for air exchange via windows” for different combinations of cases. The formula for the air quantity presented in VDI 2078 is Hansen’s approximation formula (Equation 2) and it is considering the flow through a room due to the stack effect caused by outdoor/indoor temperature differences.

$$\mathrm{Q} = 3600 * \mathrm{A_{wirk}} * \sqrt{\frac{\mathrm{g} * \mathrm{H_{wirk}} * \Delta \mathrm{T}}{2 * \mathrm{T_1}}} \tag{2}$$

Where Q is the volume flow rate [m^3/h], A_{wirk} is the effective aperture area for the flow [m^2], H_{wirk} is the effective height for the thermal updraft [m], g is the gravitational acceleration [m/s^2], ΔT is the temperature difference between inside and outside air temperature [K] and T_1 is the absolute temperature of the air flowing into the room [K]. The effective aperture area and the effective height are derived from the window’s geometric proportions and they are calculated differently, depending on the specific case: fully open window or tilted window with a maximum tilt angle of 15º and single window with inflow and outflow through the same window or windows arranged one above the other with inflow through the lower window and outflow through the upper window.

The effective aperture area and the effective height needed to calculate the volume flow rate in Equation 2 are derived from the window’s geometric proportions and have different calculation formulas depending on the specific case.

For the case “fully open window, single window with inflow and outflow through the same window” they are calculated as shown in Equation 3 and in Equation 4:

$$\mathrm{A_{wirk}} = \frac{(\mathrm{B_{li}} + \mathrm{H_{li}})}{3} \tag{3}$$

$$H_{wirk} = H_{li} * \frac{2}{3} \quad (4)$$

Where B_{li} is the width of the clear opening in the window frame [m] and H_{li} is the height of the clear opening in the window frame [m].

For the case “tilted window with a maximal tilt angle at 15º, single window with inflow and outflow through the same window” the effective aperture area and the effective height area as calculated as follows (Equations 5 and 6):

$$A_{wirk} = \frac{(B_{li} + H_{li} - H_{\varphi}) * a_{Fi-Ra}}{3} * kor_{Laib} \quad (5)$$

$$H_{wirk} = (H_{li} - H_{\varphi}) * \frac{2}{3} \quad (6)$$

Where a_{Fi-Ra} is the distance between the casement and the frame and kor_{Laib} is the correction factor for the window reveal. H_{φ} is the height of the overlap between the window frame and casement and is calculated as a fraction between a_{Falz}, the mortise depth (overlap between frame and casement) and the sinus of the opening angle (tilt angle) of the casement, φ (Equation 7):

$$H_{\varphi} \approx \frac{a_{Falz}}{\sin\varphi} \quad (7)$$

If H_{φ} is greater than H_{li}, then H_{φ} will be considered equal with H_{li}.

The distance between the casement and the frame, a_{Fi-Ra}, is calculated as follows (Equation 8):

$$a_{Fi-Ra} \approx H_{li} * \sin\varphi - a_{Falz} \quad (8)$$

If a_{Fi-Ra} results as smaller than 0, then a_{Fi-Ra} will be taken as 0. Equation 8 also gives the possibility to estimate the value of the tilt angle as shown in Equation 9:

$$\varphi \approx \arcsin\frac{(a_{Fi-Ra} + a_{Falz})}{H_{li}} \quad (9)$$

The correction factor for the window reveal is calculated as shown below, Equations 10 and10 11:

$$If\ a_{Fi-Ra} \leq a_{Laib} => kor_{Laib} = 1 \quad (10)$$

$$\text{If } a_{Fi-Ra} > a_{Laib} => kor_{Laib} = 1 - 0.6 * \left(1 - \frac{a_{Laib}}{a_{Fi-Ra}}\right) \quad (11)$$

Where a_{Laib} is the distance between the window's reveal and the casement.

The dimensions used in the previous formulas can be seen in Figure 3:

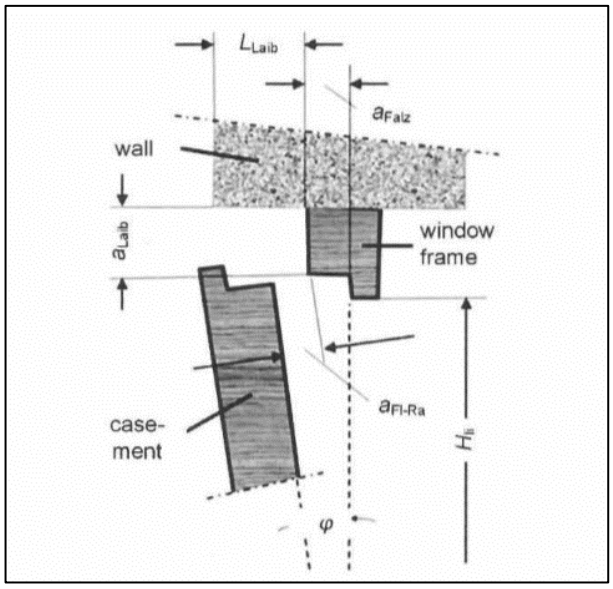

Figure 3 Diagram showing the dimensions of window frames and casements for tilted windows (source: VDI 2015)

The formula for the case of several windows at the same height in the room is as follows (Equation 12):

$$Q_T = \sum_{i=1}^{n} Q_i \quad (12)$$

Where Q_i is the air flow rate obtained through one window, calculated as in Equation 2 and Q_T is the sum of air flow rate obtained through the windows at the same height in the room.

Airflows driven by wind

Warren et al. (1985) took into consideration results from wind-tunnel experiments and full-scale experiments done in two buildings and improved the results from earlier work offering design models for both airflow driven by buoyancy in a single opening (Equation 1) and wind. The models for wind driven ventilation can be seen in Equation 13 and 14:

$$Q_w = 0.1 * A_{eff} * U_L \tag{13}$$

$$Q_w = 0.025 * A_{eff} * U_R \tag{14}$$

Where A_{eff} is the effective opening area, U_L is the local air speed at the surface of the building near the window [m/s] and U_R is the reference wind speed [m/s].

Airflows driven by temperature difference and wind

Warren (1977) investigated the effect of the turbulence in the wind at the opening and concluded that the best way to deal with a combination of buoyancy and wind effect is to calculate the airflows driven by these effects separately and then use the highest value from the two of them (Equation 15):

$$Q = max\ (Q_s\ , Q_w\ ) \tag{15}$$

De Gids and Phaff developed an empirical model from results obtained in full-scale experiments in Netherlands (De Gids and Phaff 1982). The model (Equation 16) considers the effect of both driving forces and is the recommended estimation method for the prediction of “Air flow due to window opening” in the European standard EN 15242:2007 “Ventilation for buildings – Calculation methods for the determination of air flow rate in buildings including infiltration”. (EN 2007)

$$U_m = \sqrt{C_t\ + C_w * V_{met}^2 +\ C_{st} * H_{window} * |\Delta T|} \tag{16}$$

Where C_t = 0.01 is one of the empirical coefficients [-] which takes into account the wind turbulence, C_w = 0.001 takes into account the wind speed, C_{st}= 0.0035 takes into account the stack effect, V_{met} is the meteorological wind speed at 10 m height [m/s], H_{window} is the free height of the window [m] and ΔT is the temperature difference between inside and outside air temperature [K].

The volume flow rate can be calculated as seen in Equation 17 :

$$Q_v = A_{eff} * U_m = \frac{1}{2} * A * U_m \quad (17)$$

Where Q_v is the volume flow rate [m^3/h], the factor ½ stands for the fact that the air flows in the space only through half of the window area, A [m^2] and U_m is the mean air velocity in the opening [m/s], calculated as in Equation 16.

The case of bottom hung window is also presented in the standard EN 15242:2007 which considers that the flow through the window will be only depending on the opening angle “α”. This implies that window opening area in Equation 17 will be calculated as seen in Equation 18:

$$\mathrm{A} = \mathrm{C_k}(\alpha) * \mathrm{A_W} \quad (18)$$

Where A_W is the window area (fully opened and $C_k(\alpha)$ is a polynomial approximation depending on the opening angle α. Its value can be seen in Figure 4:

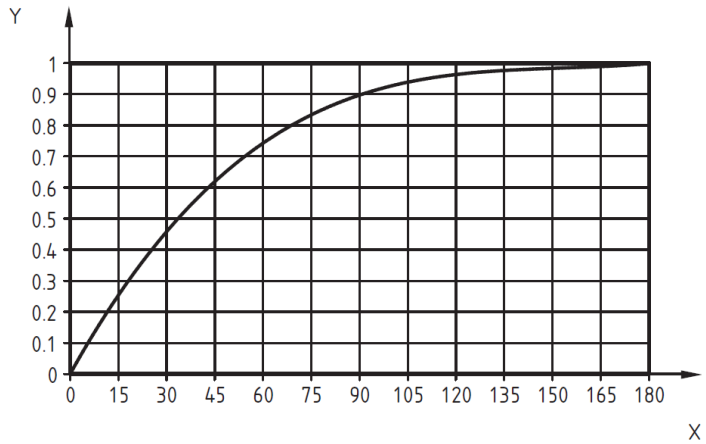

α [°]	Ck(α) [-]
0	0.00
5	0.09
10	0.17
15	0.25
20	0.33
25	0.39
30	0.46
45	0.62
60	0.74
90	0.90
180	1.00

Figure 4 Ratio of the flow through a bottom hung window and the fully open window (source: EN15242:2007)

A similar model based on several wind-tunnel and full-scale outdoor experiments was developed by Larsen (2006) as seen in Equation 19. In comparison to the other existing models, this one takes into account the influence of wind direction by using three empirical coefficients derived from the experiments. However, due to the fact that the C_D-value (discharge coefficient) used in the experiments is unknown, it is decided to consider this value as a part of the three coefficients, which makes this model valid only for openings having a similar C_D –value as the type of opening used in the experiments (Larsen 2006, Larsen & Heiselberg 2008).

$$Q_V = A * \sqrt{C_1 * |C_p| * U_{ref}^2 + C_2 * \Delta T * H + C_3 * \frac{\Delta C_{p,opening} * \Delta T}{U_{ref}^2}} \quad (19)$$

Where the constants C_1, C_2 and C_3 are empirical coefficients which depend on the wind direction and C_p is the wind pressure coefficient at the opening. The pressure differences in the opening are represented by $\Delta C_{p,opening,}$ which is expressed as an empirical function of the wind direction β as follows (Equation 20):

$$\Delta C_{p,opening} = 9.1894 * 10^{-9} * \beta^3 - 2.626 * 10^{-6} * \beta^2 - 0.0002354 * \beta + 0.113 \quad (20)$$

The ASHRAE Handbook – Fundamentals (2009) presents under the “Ventilation and Infiltration” chapter separate models for calculation of the air flow caused by wind (Equation 21) and thermal forces (Equation 22).

$$Q_w = C_V * A * U \quad (21)$$

$$Q_s = C_D * A * \sqrt{2 * g * \Delta H_{NPL} * \frac{T_i - T_o}{T_i}} \quad (22)$$

Where C_V is the effectiveness of the opening (assumed to be 0.5 to 0.6 for perpendicular winds and 0.25 to 0.35 for diagonal winds), U is the wind speed [m/s], A is the free area of the inlet opening [m^2], C_D is the discharge coefficient for the opening, ΔH_{NPL} is the height from midpoint of lower opening to the neutral plane [m], T_i and T_o are the indoor and the outdoor temperature [K].

These equations are the basis for one of the natural ventilation model ("ZoneVentilation:WindandStackOpenArea") presented in the EnergyPlus manual "Input Output Reference" (2015) which calculates the airflow rate as the quadrature sum of the wind and thermal buoyancy components (Equation 23):

$$V_{windandstack} = \sqrt{Q_s^2 + Q_w^2} \quad (23)$$

Where Q_S are Q_W the airflow rates caused by wind and by thermal forces [m^3/s].

Another model was developed in 2015 with the scope to promote ventilative cooling in the Danish revised version of the standard EN 15242:2007, called FprEN 16798-7 (Larsen et al. 2016). The model (Equation 24) is actually a modified version of the original De Gids & Phaff model (Equation 16) and is based on observations made on earlier work and experiences for the prediction of single-sided natural ventilation with a combination of thermal buoyancy and wind:

$$q_{V;arg} = 3600 * \frac{\rho_{a;ref}}{\rho_{a;e}} * \frac{A_{w;tot}}{2} \max\left(C_{wind} * u_{10;site}^2 ; C_{st} * h_{w;st} * abs(T_z - T_e)\right)^{0.5} \quad (24)$$

Where $q_{V;arg}$ is the airflow through the window [m^3/h], $\rho_{a;ref}$ and $\rho_{a;e}$ are the reference and external air densities [kg/m^3], $A_{w;tot}$ is the total window opening area [m^2], C_{wind} is the wind speed coefficient [-], $h_{w;st}$ is the useful stack effect height for airing [m], *'Tz - Te'* is the temperature difference between the ventilation zone and the outdoor air [K].

As the original model showed in many experiments an overestimation of air flow rates at low wind speeds and low temperature differences, the new formula aimed to predict air flow rates through windows by being on a safe side as it was intended to be used in standards. Therefore, an underestimation of the air change rates was preferred. A modification was to remove the wind turbulence coefficient C_t (as seen in Equation 24) because of its positive air flow contribution at low wind speeds and at very low temperature differences. The removal of this constant was also done for the case of single-sided ventilation in the RT2012 which is the French thermal standard (Plesner et al. 2015). Another modification was to consider the highest value from the two effects (wind and stack effect) in the model, which corresponds to the former conclusions of Warren and Parkins (1985).

In addition, in some cases, engineering offices dealing with the calculation of the ventilation systems calculation and evaluation of thermal comfort in different spaces use their own simple methods/models of estimating window ventilation. For example, the engineers at Drees and Sommer Advanced Building Technologies in Munich use the following set of equations (Equations 25, 26, 27, 28 and 29) to estimate the air flow rates caused by window ventilation in [1/h]:

$$\text{If } T_{ext} <= -5° => ACR_1 = 1 \quad (25)$$

$$\text{If } -5° < \mathrm{T}_{ext} <= 18° => ACR_2 = 1 + 2 * (T_{ext} + 5)/(18 + 5) \quad (26)$$

$$\text{If } 18° < T_{ext} <= 26° => ACR_3 = 4 \quad (27)$$

$$\text{If } 26° < \mathrm{T}_{ext} <= 32° => ACR_4 = 3 - 2 * (T_{ext} - 26)/(32 - 26) \quad (28)$$

$$\text{If } T_{ext} > 32° => ACR_5 = 1 \quad (29)$$

The set of equations are based on the assumption that in winter and summer, at extreme low and high temperatures, a space will be ventilated with a lower air change rate, whereas at pleasant outside temperatures higher air exchange rates are assumed. The set of equations estimates as a function of outside temperature a maximal air change rate with values between 1 and 4 [1/h] (Equation 30). It is also assumed that at a lower temperature difference between inside and outside, the maximal air change rate will not be reached, therefore a reduced air exchange rate will be estimated (Equation 31).

$$\mathrm{ACR_s} = \mathrm{ACR_1} + \mathrm{ACR_2} + \mathrm{ACR_3} + \mathrm{ACR_4} + \mathrm{ACR_5} \quad (30)$$

$$\mathrm{ACR} = \max(\mathrm{ACR_s}, \sqrt{|\mathrm{T_i} - \mathrm{T_o}|}) \quad (31)$$

1.3.5 Measurements of air change rates with tracer gas

Air change rates can be measured using tracer gas measurements in a number of variations: Decay or growth method, constant concentration method, constant injection method. These techniques are described in several standards: ASTM E741

Standard Test Method (2011), ISO 12569 (2012) and VDI 4300, part 7 (2001). In general, the measurements consist of releasing an amount of gas in a monitored space which is then used in determining the air change rate as a function of time. This kind of measurements is involves complex procedures and require relatively intensive prior preparations to succeed.

The tracer gases should be inert, non-reactive, and unharmful for the environment and the occupants in the studied space. The tracer gas shall not exist in the constituents of air and if possible should be easy to measure and inexpensive (Sherman 1990; Raatschen 1995). Nevertheless, no tracer gas can accomplish all these requirements. As Raatschen (1995) mentions, in past studies different tracer gasses were used, such as hydrogen, helium, oxygen, carbon monoxide, methane, acetone, but these gases are not considered ideal tracer gases.

The following tracer gases are commonly used nowadays in practice (Laussmann and Helm 2004): Sulphur hexafluoride (SF_6), Nitrous oxide (N_2O) and halogenated hydrocarbons, like hexafluorobenzene (C_6F_6) and perfluorocarbons (PFC). Still, these gases have a high greenhouse effect and they are also an expensive solution. Additionally, the nitrous oxide is toxic at low concentration level and the other gases have a high density compared to air, which does not make them ideal as tracer gas.

However, SF_6 is commonly used in these kind of measurements since it offers reliable results.

Carbon dioxide (CO_2) can also be a good solution since it fulfills many of the requirements of an ideal tracer gas: it is non-toxic and non-reactive at low concentrations, it has a close density to that of the air and it is an inexpensive solution (Cui et al. 2015). Moreover, it is easier nowadays to measure CO_2 levels with low-cost, but still high-performance sensors available on the market than with a sampling systems and gas analyzer. Cui et al. (2015) proved in their study that the use of CO_2 sensors in the tracer gas measurements offers the same performance as the classical sampling method of determining the air change rate. Using CO_2 as a tracer gas can be made either by releasing it in a room via a gas container or by analyzing the CO_2 indoor emissions caused by people's presence (Persily 1996; Persily 1997; Laussmann & Helm 2011a). Persily (1997) describes in his work the evaluation of building ventilation via occupant-generated carbon dioxide and also addresses the issues of carbon dioxide measurements. For example, it has to be taken into consideration that the outdoor concentration of CO_2 is not 0, by replacing the indoor concentration in the calculations with the difference between the indoor and the

outdoor concentrations. There are numerous studies in which the occupants-generated CO_2 concentration level is used to evaluate the ventilation in a space (Laussmann and Helm 2011, Yan et al. 2007, Benedettelli et al. 2015). However, one must understand that using occupants-generated CO_2 concentrations in determining air change rates is highly dependent on the occupancy patterns of the respective building (Persily 1997).

1.4 Hypothesis

Given the literature review presented in the previous chapters, this thesis addresses the following research questions in order to test the reliability of the studied methods: How does the ventilation air change estimations differ from measured values in a specific case? To which extent are the methods influenced by outside meteorological conditions and which parameters influence the results? Are the calculation methods present in the current standards able to offer a quick and reliable estimation of air change rates through window ventilation for building designers? The present thesis will deal with the performance of existing calculation methods for single sided ventilation air change rate in comparison with measurement data.

2 METHOD

2.1 Overview

The focus of this research is to evaluate different existing calculation methods of the single sided ventilation air change rates. After a literature review five widely-used methods for estimation of air change rate were selected to be analyzed. The verification and validation of the models was done through full-scale measurements in a university in Wien, Austria.

In this chapter, besides description of the selected methods, the specific study cases and their influencing parameters are described. Also, the buildings and the measurement with two different tracer gases are described and illustrated. The position and technical data of the sensors and equipment is also presented. The collected data is referring to indoor and outdoor environment (temperature, relative humidity, tracer gas concentrations, wind speed and direction).

2.2 The Selected Single-Sided Calculation Methods

Implementing natural ventilation in a building could offer significant energy savings. However, its effectiveness is highly dependent on the climatic conditions, more specifically on the wind speeds and temperature differences across the opening. Choosing between different calculation methods for natural ventilation depends on the different levels of the design process. For this reason, it makes sense at an early stage of the design process, when different parameters of the building are still uncertain, to use analytical models for predicting the air flows for simple and single-zone geometries. Design models for natural ventilation could offer a quick and simple estimation of the effectiveness of the ventilation design strategies by predicting the airflows through window openings.

Five different calculation methods were selected to be analyzed, as seen in

Table *2*: the models proposed by Warren and the one proposed by De Gids & Phaff, Hansen's approximation formula, the calculation methods for natural ventilation presented in the ASHRAE's Handbook and the calculation method used in an engineering office.

Table 2 Selected existing calculation methods for the estimation of airflow rate in single-sided ventilation

Nr. crt.	Calculation Methods	Stack effect	Wind effect	Combination of Stack and Wind effects
1	Warren	$Q_s = \frac{1}{3} * A * C_d * \sqrt{\frac{\Delta T * H * g}{T_{ave}}}$	$Q_w = 0.025 * A_{eff} * U_R$	$Q = max\ (Q_s, Q_w)$
2	De Gids & Phaff (EN 15242)			$Q_v = A_{eff} * U_m = \frac{1}{2} * A * U_m$ $U_m = \sqrt{C_t + C_w * V_{met}^2 + C_{st} * H_{window} * \lvert\Delta T\rvert}$
3	Hansen (VDI 2078)	$Q = A_{wirk} * \sqrt{\frac{g * H_{wirk} * \Delta T}{2 * T_1}}$		
4	ASHRAE HoF	$Q_s = C_D * A * \sqrt{2 * g * \Delta H_{NPL} * (T_i - T_o)/T_i}$	$Q_w = C_V * A * U$	$Q_{windandstack} = \sqrt{Q_s^2 + Q_w^2}$
5	DS Method	If $T_{ext} <= -5° => ACR_1 = 1$ If $-5° < T_{ext} <= 18° => ACR_2 = 1 + 2 * (T_{ext} + 5)/(18 + 5)$ If $18° < T_{ext} <= 26° => ACR_3 = 4$ If $26° < T_{ext} <= 32° => ACR_4 = 3 - 2 * (T_{ext} - 26)/(32 - 26)$ If $T_{ext} > 32° => ACR_5 = 1$ $ACR_s = ACR_1 + ACR_2 + ACR_3 + ACR_4 + ACR_5$ $ACR = max\ (ACR_s, \sqrt{\lvert T_{int} - T_{ext}\rvert})$		

Warren's research work has been mentioned and analyzed in several scientific papers, showing in most cases results with good agreement to measurements (Yamanaka et al. 2006, Larsen 2006, Zhai et al. 2015, Caciolo et al. 2011). In 1985, Warren and Parkins (Warren et al. 1985) improved the equations developed by Warren from his earlier work and experiments (Warren 1977). The models for the volume flow rate which are also studied in the present thesis are the model for the stack effect based on analytical considerations (Equation 1) and model for the wind effect based on experiments (Equation 14). As Warren concluded, the best way to deal with the combination of the two effects is to calculate them separately and use the highest value of the two as presented in Equation 15.

The next studied model in this thesis is the one proposed by De Gids and Phaff obtained from 33 full-scale measurements and valid for the combination of wind and stack effects (Equation 16). The calculation method is also recommended in the European standard EN 15242:2007 "Ventilation for buildings – Calculation methods for the determination of air flow rate in buildings including infiltration" for the prediction of "Air flow due to window opening".

The third calculation method is the one presented in VDI 2078 Standard "Calculation of thermal loads and room temperatures". Annex A3 of the mentioned standard offers an "Approximation Formulae for air exchange via windows" for five different cases:

fully open window or tilted window, at maximum angle of 15º, as single window with inflow and outflow through the same window or as windows arranged one above the other, with inflow through the lower window and outflow through the upper window. The fifth case is the case with several windows at the same height in the room. The formula (Equation 2) for the air quantity presented in VDI 2078 is Hansen's approximation formula and it is considering the flow through a room due to the stack effect caused by outdoor/indoor temperature differences (Verein Deutscher Ingenieure-Fachbereich Technische Gebäudeausrüstung 2015). The studied cases in the present thesis for the effective opening area are: "fully open window, single window with inflow and outflow through the same window", "tilted window with a maximal tilt angle at 15º, single window with inflow and outflow through the same window" and "several windows at the same height in the room".

The fourth selected calculation method are the models presented in ASHRAE Handbook – Fundamentals (2009), which presents separate equations for estimation of the air flow caused by wind (Equation 21) and stack effect (Equation 22). These equations are also presented in the EnergyPlus "Input Output Reference" manual (2015) for the natural ventilation model ("ZoneVentilation:WindandStackOpenArea"), where the air flow rate is considered as a function of both wind speed and thermal stack effect and is calculated as the quadrature sum of the wind and thermal buoyancy components (Equation 23).

The last studied model is a model proposed by engineers from the company Drees & Sommer Advanced Building Technologies, here referred to as the 'DS Method'. The model consists of a set of equations (Equations 25, 26, 27, 28 and 29), which computes the air change rate with values between 1 and 4 [1/h] as a function of exterior air temperature as previously shown in Chapter 1.3.4. Thereby, it is assumed that during extreme outside temperatures (in winter time and summer time), the air change rate has lower values as compared with periods with pleasant temperatures, in which there is a greater probability of opening the window, thus the air change rate can reach higher values.

The selected methods consider different driving forces and are influenced by different parameters, as presented in Table 3. Also different cases of window opening are considered in this research, from fully open to half open and tilted. The window settings scenarios together with their names used in the present work are shown in Table 4.

Table 3 Influencing parameters of the selected existing calculation methods

Nr. crt.	Calculation Methods	Influencing Parameters
1	Warren	- A – effective area of the opening [m^2] - H – free height of the window [m] - T_{int} & T_{ext} – interior and exterior temperature [K] - C_d – discharge coefficient [-] - U_R – reference wind speed [m/s]
2	De Gids & Phaff (EN 15242)	- A_{eff} – effective area of the window [m^2] - H_{window} – free height of the window [m] - T_{int} & T_{ext} – interior and exterior temperature [K] - v_{met} – meteorological wind speed at 10 m height [m/s]
3	Hansen (VDI 2078)	- A_{wirk} – effective area of the window [m^2] - H_{wirk} – effective height of the window [m] - T_{int} & T_{ext} – interior and exterior temperature [K]
4	ASHRAE HoF	- A – free area of the window [m^2] - H_{NPL} – height from midpoint of lower opening to the neutral plane [m] - T_{int} & T_{ext} – interior and exterior temperature [K] - C_D – discharge coefficient [-] - U – wind speed [m/s] - C_V – effectiveness of the opening coefficient given by the wind direction [-]
5	DS Method	- T_{int} & T_{ext} – interior and exterior temperature [K]

Table 4 Window settings scenarios used in the measurements

Nr. crt.	Window settings scenarios	Scenario name
1	Window 1 – Half open	W1_HO
2	Window 1 – Fully open	W1_FO
3	Window 2 – Half Open	W2_HO
4	Window 2 – Fully open	W2_FO
5	Window 1 and 2 – Half open	W1_W2_HO
6	Window 1 and 2 – Fully open	W1_W2_FO
7	Window 1 – Tilted	W1_T
8	Window 2 - Tilted	W2_T

Another important aspect considering the case for tilted window is that only two of the methods from the five studied methods offer extra formulas for the area of the opening in the case of tilted window, namely the Annex A3 of the VDI 2078 Standard (VDI 2015) and the European standard EN 15242:2007 (EN 2007) . In order to see how the other methods would perform in the case of tilted window, the window opening areas used in the specified two methods were applied to the other methods.

2.3 Tracer Gas Measurements

2.3.1 Description of Measurements

The air change rates via window ventilation were measured with the tracer gas decay method by using SF6 as a tracer gas. An amount of tracer gas SF_6 was injected for 10 seconds from a gas cylinder with a pressure reducer and mixed into the air in the room with the help of a ventilator. The gas concentration was measured with a gas analyzer at regular time intervals (30 sec) and when it reached a constant value between 70-80 ppm, the ventilator was switched off and the window was opened. Then the decrease of the tracer gas concentration began and the values were recorded until the gas concentration reached a lower value, between 1-10 ppm, when the measurement ended. A schematic illustration of the concentration of the tracer gas and the exponential decay can be seen in Figure 5a. Figure 5b shows that by plotting the natural logarithm of a gas concentration against time a straight line is obtained. The gradient of that line is the air change rate in the room, calculated as shown in Equation 32:

$$N = \frac{ln\, C(0) - ln\, C(\tau_1)}{\tau_1} \tag{32}$$

Where *C(0)* and *C(τ)* are the tracer gas concentrations at the initial and final point of the decay curve and τ_1 is the time difference between the end of the measurement and the beginning of the concentration decay.

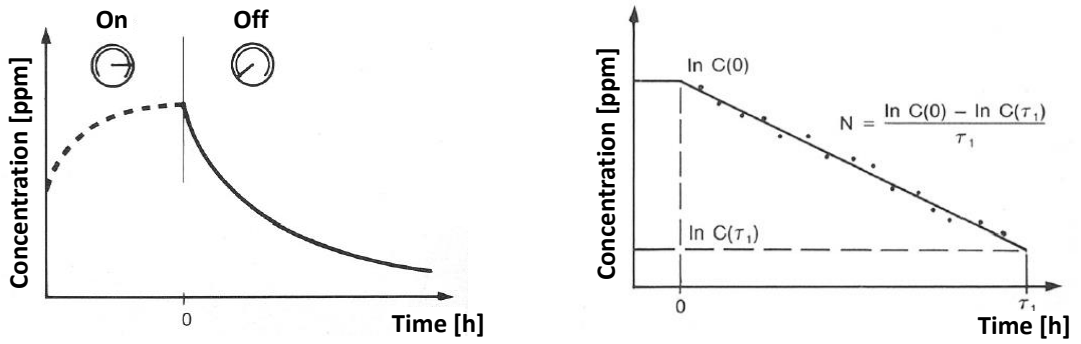

a) Concentration decay

b) Calculation of air change rate

Figure 5 a) The decay of the tracer gas concentration and b) Calculation of air change rate (source: "Building Monitoring and Diagnostics" lecture notes, TU Wien)

The external conditions were measured with a weather station positioned on the top of the building and the internal conditions were measured with the help of two temperature loggers.

The studied cases for the purpose of this thesis were of single-sided ventilation with different window setups: one fully open window, one tilted window and fully open window with 2 windows on the same side and height in the room. In order to observe how the area of the opening affects the air change rate, the case with fully open window for the specific study case in this work was realized considering the clear area of the opening when only one window pane was open, but also the clear area of the opening when both window panes are open. These cases can be later identified as “half open” and “fully open”. An overview of the studied window settings scenarios can be seen in Table 4.

2.3.2 The test room

Tracer gas technique has been used during this research in order to measure the air change rate through single-sided ventilation. The experiments were made during the summer of 2017 in a seminar room of the Department of Building Physics and Building Ecology at Vienna University of Technology (Figure 6), Austria. The room situated on the 4th floor is referred here as “the test room”.

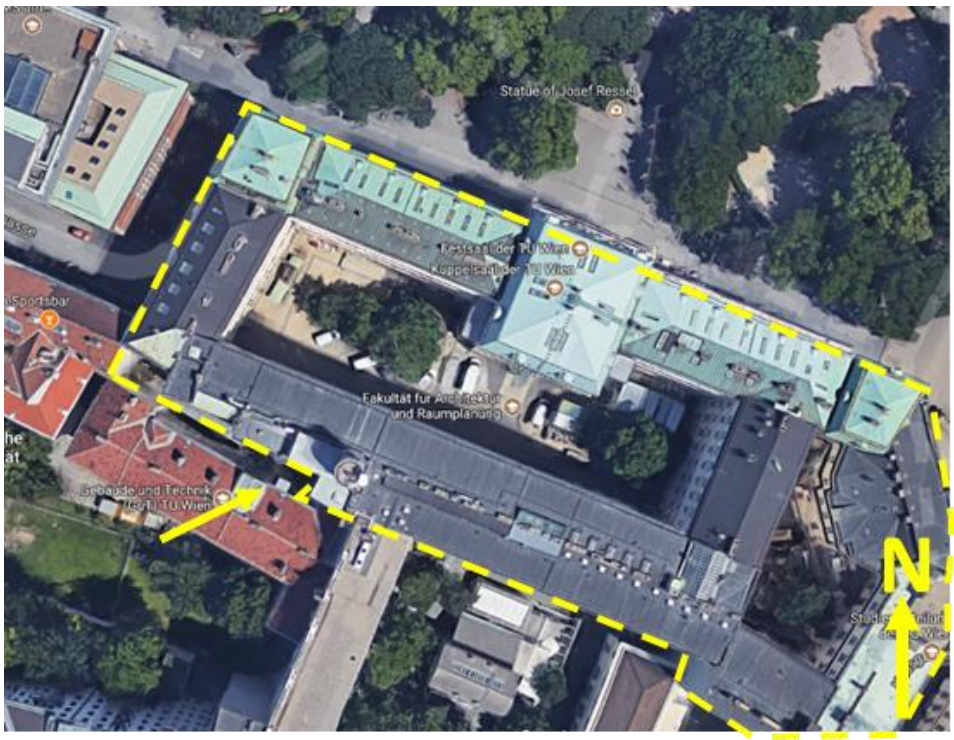

Figure 6 The test room at TU Wien (source: Google Maps)

The dimensions of the room are 2.35 x 7.46 m with a room height of 2.58 m, which gives a total room volume of 45.23 m^3 (Figure 7).

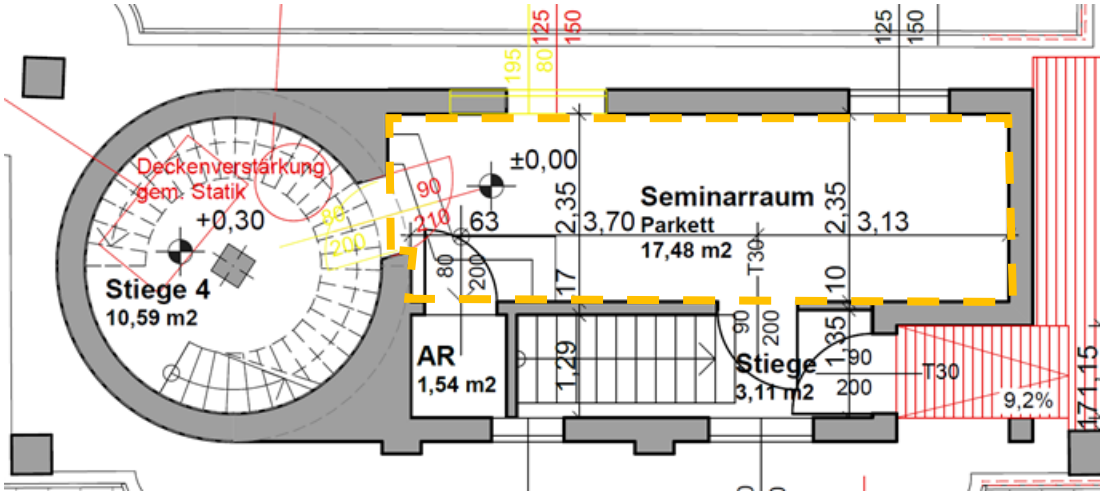

Figure 7 Schematic plan of the test room (source: Department of Building Physics and Building Ecology, TU Wien)

In the room there are two windows on the same side and at the same height. The size of each opening is 1.25 x 1.50 m, both oriented towards SW. The free area of the window is 1.45 m^2 (1.08 x 1.34 m). The position of the openings in the exterior wall is shown in Figure 7 and Figure 8.

Figure 8 Position of the two windows of the test room on the façade of TU Wien (Source: Google Maps)

The tracer gas measurements with SF_6 as tracer gas were performed in August 2017. Since there were two operable windows available on the same side in this room (W1 and W2), variations of opening state (fully open, half open, tilted) were considered for each window. The cases with both windows fully open and half open were also analyzed.

2.3.3 External parameters

In order to measure outdoor climatic conditions like temperature [°C], wind speed [m/s] and wind direction [degree] the existing weather station of the Department of Building Physics and Building Ecology mounted on the top of the roof was used (Figure 9).

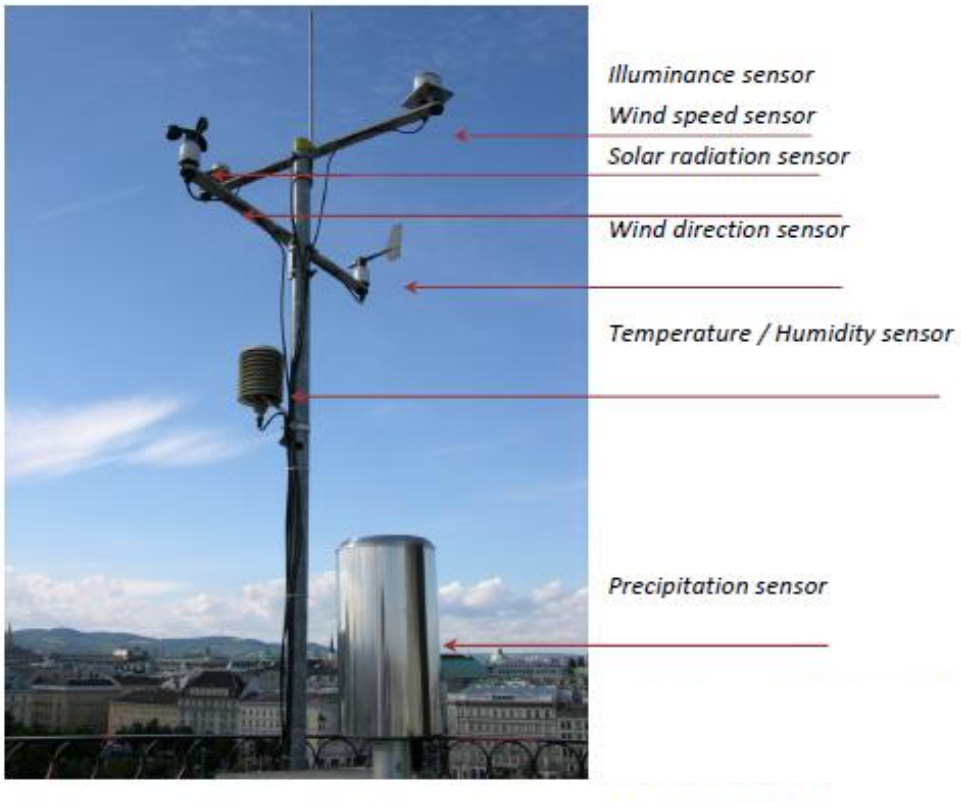

Figure 9 WSBPI Weather station mounted on the roof of TU Wien (source: Pröglhöf 2009)

The weather station manufactured by Adolf Thies GmbH & Co.KG is connected to the local network and can also measure the solar radiation [W/m^2], relative humidity [%], atmospheric pressure [Pa], outdoor illuminance [lx] and precipitation [mm]. Its sensors transmit analog signals to a data logger which generates output files that are processed into <*.txt> files, which are then stored. The local weather data is structured in 30 seconds intervals.

2.3.4 Internal parameters

The internal parameter which was of great interest for the experiments was the indoor air temperature. In order to obtain an accurate value, two sensors were installed in the room at different positions (Figure 9) and the mean average value was later used in the calculations. The sensors used for the measurements were air quality sensors THERMOKON SR04 CO2rHLCD (Figure 10) which can measure different parameters such as indoor air temperature, CO_2 level and relative humidity.

Figure 10 Temperature loggers mounted in the test room

To perform the tracer gas measurements a gas analyzer, a gas cylinder containing sulfur hexafluoride (SF_6) with pressure reducer and a ventilator were used (Figure 11).

Figure 11 Gas analyzer, SF_6 gas cylinder with pressure reducer and ventilator

The schematic plan of the test room at TU Wien with the position of the windows and the sensors can be seen in Figure 12.

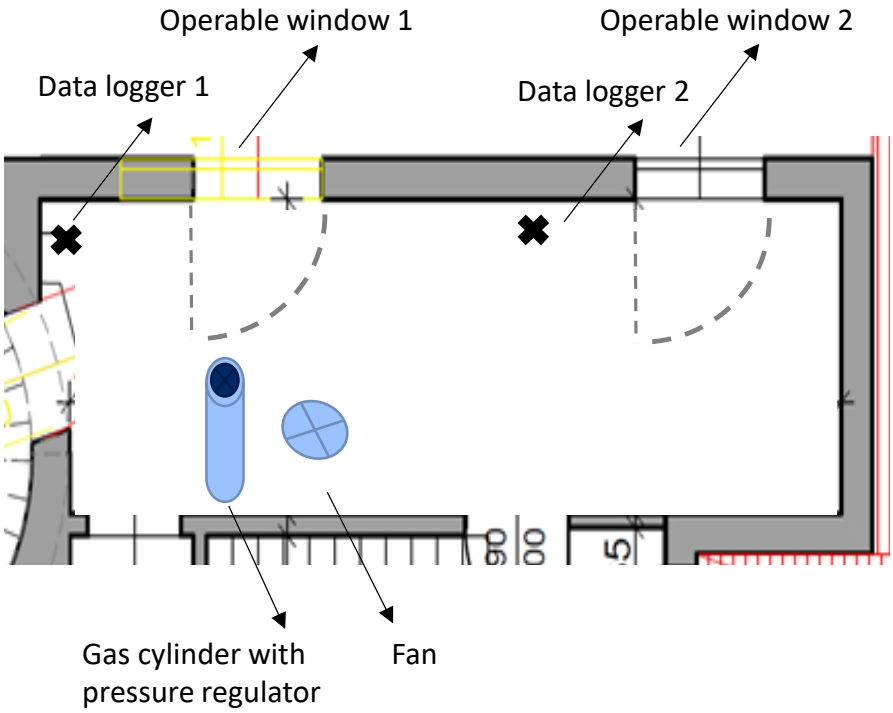

Figure 12 Schematic plan of the test room with position of sensors

2.3.5 Measurements during a test session

The following steps were made during a test session of tracer gas measurements with SF6:

1. The ventilator was tuned on (level 3)
2. The SF_6 was released in the room for 10 sec at 0.5 bar
3. When the SF_6 concentration reached a constant level in the room (around 70 - 80 ppm) the windows was open according to the studied case and the ventilator was switched off.
4. The experiments were ended when the SF_6 concentration in the room dropped to around 5 ppm

2.4 Data processing and calculations

The data sets of the performed measurements included data of interior and exterior parameters. To start the data processing, all measurements were checked and then put in Excel sheets. Next, the different sets of data were sorted into separated sheets for each studied window setting scenario and the measured air change rate was calculated.

Further, an excel tool containing the studied calculation methods together with their influencing parameter was created. An overview of how the excel tool was structured can be seen in Figure 13.

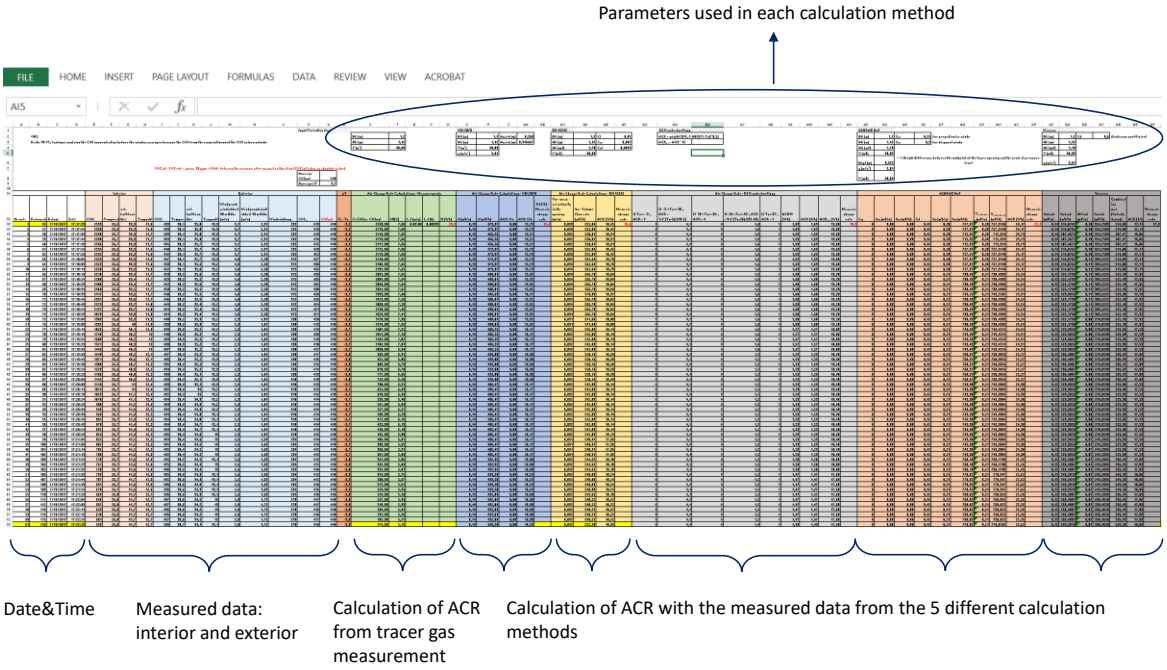

Figure 13 Screenshot of the excel tool created for the calculations of the studied calculation methods of single sided ventilation

3 RESULTS AND DISCUSSION

3.1 Measured air change rates

After performing the measurements as described in Chapter 2.3.1 the air change rate was calculated from the decay of the tracer gas concentration. Figure 14 shows the concentration decay and the determination of the air change rate through the logarithmic scale of the gas concentration in the measurement case of “window 2 half open”.

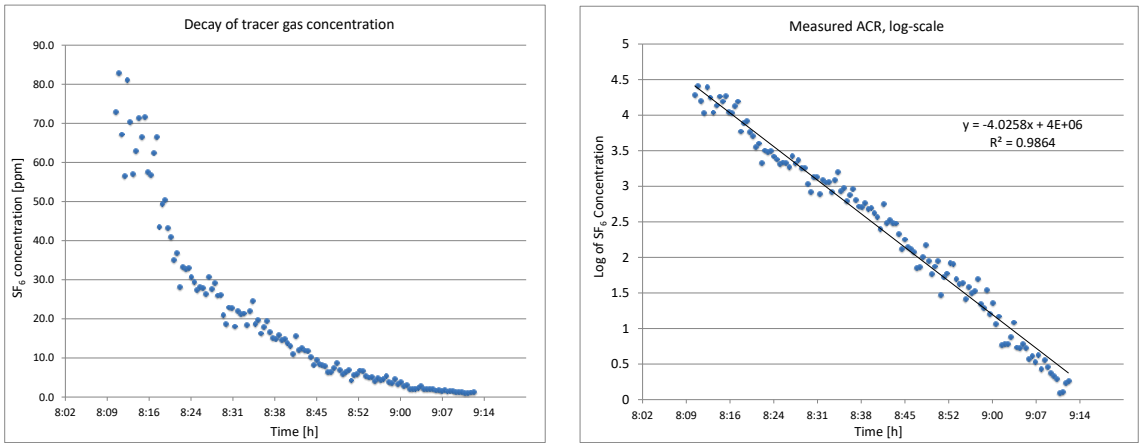

Figure 14 Concentration decay for the measurement case “window 2 half open”; in linear scale (left), and in logarithmic scale (right) together with the linear regression and the air change rate as the decay coefficient

The next two figures also show the determination of air change rate from the SF_6 concentration decay for the measurement cases of “window 2 fully open” as seen in Figure 15 and “window 2 tilted” as seen in Figure 16. Analyzing the figures of the concentration decays in the three different cases, it can be it can be observed how fast the SF_6 concentration decays in the case of higher opening area.

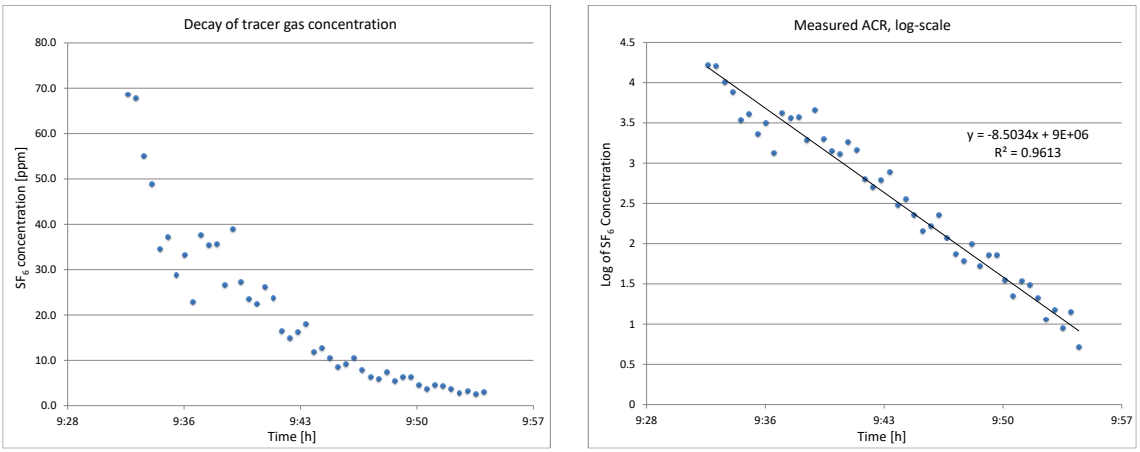

Figure 15 Concentration decay for the measurement case "window 2 fully open"; in linear scale (left), and in logarithmic scale (right) together with the linear regression and the air change rate as the decay coefficient

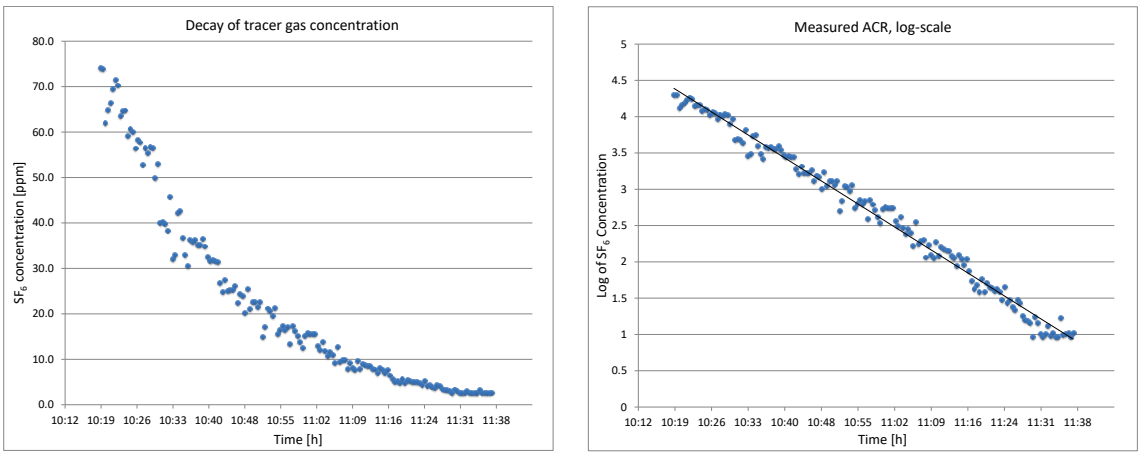

Figure 16 Concentration decay for the measurement case "window 2 tilted"; in linear scale (left), and in logarithmic scale (right) together with the linear regression and the air change rate as the decay coefficient

Table 5 shows the measured boundary conditions and air changes rates for all the studied cases. As specified before, the measurements were made during the summer period in August 2017 in a time period with high temperatures both inside and outside. The temperature difference between inside and outside air was always below 5 K. Therefore, it can be said that the following discussions on the differences between ventilation air change estimations and measured values are valid only for this specific cases with extreme summer temperatures.

An aspect that draws attention is the fact that the measurement for the case of "window 2 fully open" gives an air change rate of almost double as in the case of "window 1 fully open" despite the fact that the opening area is the same and that the

values of ΔT are not that far from each other. First of all, it can be observed that the wind speed has a significant influence on the air change rate. Second of all, it needs to be mentioned that when the measurement for “window 2 fully open” was made the wind was blowing directly into the test room and in the situation of “window 1 fully open” the wind was blowing towards the opposite side of the building. Thus, it can be argued that the wind direction also has a strong influence on the air change rates.

It can also be observed that the cases number 5 and 6 when both windows in the test room were open, first half open and then fully open, give extreme values of air change rates. From a first look it can be seen that the measured boundary conditions, namely the temperature difference between outside and inside air and the wind speed, have much higher values as in the other cases. Also, the measurement setup for these two cases by having two windows open and the shape of the room could have led to high velocities of the inside air, therefore causing the exchange of the air in the room much faster and resulting in very high air change rates. Case number 6 is particularly unclear given the high wind speed and the fact that the wind was predominantly blowing from SE, thus blowing constantly into the room during the measurements. Given these uncertainties, it was decided to exclude case number 6 from the further analyses.

Table 5 Measured boundary conditions and air change rates in the test room the air change rate

Measurement number	Window setup	Boundary conditions				ACR values [h^{-1}]
		Ti,ave [K]	To,ave [K]	|ΔT| [K]	Average Wind Speed [m/s]	Measured
1	W1_HO	31.9	33.3	1.4	2.2	4.5
2	W1_FO	31.7	31.1	0.6	2.4	4.6
3	W2_HO	30.9	30.6	0.3	3.5	4.0
4	W2_FO	31.3	32.3	1.0	3.8	8.5
5	W1_W2_HO	32.3	36.5	4.2	4.7	21.9
6	W1_W2_FO	33.2	37.2	4.0	6.1	43.1
7	W1_T	32.6	35.4	2.8	4.7	3.1
8	W2_T	31.8	34.5	2.6	3.7	2.6

The air change rates determined from the measurements and their comparison to the air change rates determined from the selected empirical models will be further discussed in section 3.2.

3.2 Calculated air change rates

In the following sections the measured and the calculated air change rates for the eight different cases will be presented together with interpretations and discussion of the results.

3.2.1 Hansen's method (VDI 2078)

Table 6 shows the results obtained with the estimation method offered by the VDI 2078 Standard "Calculation of thermal loads and room temperatures" previously presented in section 1.3.4. This standard treats window ventilation as updraft-induced thermal natural ventilation, so the influencing parameters in this case are the temperature differences and the window's dimensions. When comparing the cases of window 1 and window 2, firstly the two cases when each is half open and then each fully open, it can be seen that when temperature differences are higher the estimated air change rates are also higher. Whereas when comparing the cases for window 1 half open and window 1 fully open, it can be seen that the model reacts more to the area of the opening than to the temperature differences. In general, this method returns values which are lower than the measured values in these specific cases. This might happen because the model does not take into account the effect of the wind considering that when the measurements were done the temperature difference was not that high in comparison to the wind speed which had higher values.

Table 6 Estimations of air change rate offered by Hansen's (VDI 2078) calculation method

Measurement number	Window setup	Boundary conditions				ACR values [h^{-1}]	
		Ti,ave [K]	To,ave [K]	|ΔT| [K]	Average Wind Speed [m/s]	Measured	Hansen (VDI 2078)
1	W1_HO	31.9	33.3	1.4	2.2	4.5	2.6
2	W1_FO	31.7	31.1	0.6	2.4	4.6	3.5
3	W2_HO	30.9	30.6	0.3	3.5	4.0	1.2
4	W2_FO	31.3	32.3	1.0	3.8	8.5	4.6
5	W1_W2_HO	32.3	36.5	4.2	4.7	21.9	9.0

3.2.2 De Gids and Phaff's method (EN 15242)

Table 7 presents the air change rates calculated with the De Gids and Phaff model which is also proposed in the European standard EN 15242:2007 "Ventilation for buildings – Calculation methods for the determination of air flow rate in buildings including infiltration" as presented in section 1.3.4. The influencing parameters of this

method are the temperature differences and the window's dimensions, but also the wind speed. When looking at the cases of window 1 and window 2 and comparing the results offered by the different setups of half and fully open it can be seen that this model also reacts to the size of the opening, considering that the average wind speed had similar values when the area of the opening was changed. The model returns reasonable results in the case of a smaller opening.

Table 7 Estimations of air change rate offered by De Gids & Phaff's (EN 15242) calculation method

Measurement number	Window setup	Boundary conditions				ACR values [h^{-1}]	
		Ti,ave [K]	To,ave [K]	|ΔT| [K]	Average Wind Speed [m/s]	Measured	De Gids & Phaff (EN 15242)
1	W1_HO	31.9	33.3	1.4	2.2	4.5	4.0
2	W1_FO	31.7	31.1	0.6	2.4	4.6	7.8
3	W2_HO	30.9	30.6	0.3	3.5	4.0	4.2
4	W2_FO	31.3	32.3	1.0	3.8	8.5	9.8
5	W1_W2_HO	32.3	36.5	4.2	4.7	21.9	12.5

3.2.3 DS method

Table 8 gives the air change rates calculated according to the "DS Method" which involves a set of equations which computes the air change rate with values between 1 and 4 [1/h] as a function of exterior air temperature as explained in section 1.3.4. These method is used in thermal simulations by an engineering company. The parameters influencing the equations are only the outside air temperature and the temperature difference as it can also be seen in the results. Nevertheless, an underestimation of the air change rates is observed.

Table 8 Estimations of air change rate offered by the DS Method

Measurement number	Window setup	Boundary conditions				ACR values [h^{-1}]	
		Ti,ave [K]	To,ave [K]	|ΔT| [K]	Average Wind Speed [m/s]	Measured	DS Method
1	W1_HO	31.9	33.3	1.4	2.2	4.5	3.6
2	W1_FO	31.7	31.1	0.6	2.4	4.6	1.6
3	W2_HO	30.9	30.6	0.3	3.5	4.0	0.6
4	W2_FO	31.3	32.3	1.0	3.8	8.5	2.6
5	W1_W2_HO	32.3	36.5	4.2	4.7	21.9	9.2

3.2.4 ASHRAE HoF method

Table 9 shows the air change rates calculated with the equations given by the ASHRAE's Handbook. Like explained in section 1.3.4 of this thesis, in the handbook are two separate equations given for air flows caused by the stack effect and air flows caused by the wind effect only. The combination of the two effects was calculated as presented in the EnergyPlus manual "Input Output Reference" (2015) which calculates the airflow rate as the quadrature sum of the wind and thermal buoyancy components (Equation 23).

Table 9 Estimations of air change rate offered by ASHRAE HoF method

Measurement number	Window setup	Boundary conditions				ACR values [h^{-1}]			
							ASHRAE HoF		
		Ti,ave [K]	To,ave [K]	|ΔT| [K]	Average Wind Speed [m/s]	Measured	ASHRAE HoF Stack	ASHRAE HoF wind	ASHRAE HoF comb.
1	W1_HO	31.9	33.3	1.4	2.2	4.5	3.9	25.7	27.2
2	W1_FO	31.7	31.1	0.6	2.4	4.6	5.2	83.2	83.3
3	W2_HO	30.9	30.6	0.3	3.5	4.0	1.8	59.0	59.2
4	W2_FO	31.3	32.3	1.0	3.8	8.5	6.8	124.5	125.6
5	W1_W2_HO	32.3	36.5	4.2	4.7	21.9	13.8	119.7	124.4
6	W1_W2_FO	33.2	37.2	4.0	6.1	43.1	28.2	419.6	420.6

It can be observed from Table 9 that the high values of the air change rates calculated as the combination of the effects are actually caused by the case of air flows caused by the wind effect. As in all of the cases the wind was blowing towards the test room, it can be seen how it influenced the results. The parameter which strongly influences these results is $C_{V,}$ the effectiveness of the opening which in this work is assumed to be 0.55 for perpendicular winds and 0.3 for diagonal winds, same as in the EnergyPlus manual "Input Output Reference" (2015). The manual references the ASHRAE Handbook – Fundamentals (2009) for the values of the effectiveness of the opening (C_V), where C_V is assumed to be between 0.5 to 0.6 for perpendicular winds and 0.25 to 0.35 for diagonal winds. In order to see how this coefficient influences the results of the ASHARE HoF calculation method for the wind effect only, a few variations were made as shown in Table 10. Considering that during the measurements the wind was predominantly diagonal three values of the effectiveness of the opening were used in the calculation method for the specific measurement cases to see the influence on the air change rates. The value 0.55 for C_V was also used assuming a situation of the wind being predominantly perpendicular. It can be clearly seen that the model reacts strongly to this coefficient, resulting in high and unrealistic estimations of air change rates. Moreover, there is no value given or other

specification for the case of the wind blowing on the leeward side of the building, which although would not have a strong influence on the air change rate it might still have a small influence and should be considered in calculations. An adjustment of this coefficient could improve the performance of this model.

Table 10 Influence of the C_V coefficient on the air change rates for the specific measurement cases (ASHRAE HoF Wind)

Nr.			ACR values [h-1] - ASHRAE HoF Wind				
crt.	C_V [-]	Wind direction	W1_HO	W1_FO	W2_HO	W2_FO	W1_W2_HO
1	0.25	Diagonal winds	21.4	69.3	50.6	106.5	99.7
2	0.3		25.7	83.2	59.0	124.0	119.7
3	0.35		30.0	97.0	67.4	142.6	139.0
5	0.55	Perpendicular winds	47.1	152.5	101.1	214.9	219.4

In addition the influence of the wind speed on the calculation method for the wind only offered by ASHRAE HoF was also investigated. Since during the measurements there were wind velocities between 1 – 6 m/s recorded, the same values was used for the variation of the average wind speed for the specific study cases as it can be seen in Table 11.

Table 11 Influence of the wind velocity on the air change rates for ASHRAE HoF wind

Nr.	Wind Velocity	ACR values [h-1] - ASHRAE HoF Wind				
crt.	[m/s]	W1_HO	W1_FO	W2_HO	W2_FO	W1_W2_HO
1	1	11.5	34.6	16.8	32.6	25.4
2	2	23.0	69.1	33.6	65.3	50.7
3	3	34.5	103.7	50.4	97.9	76.1
4	4	45.9	138.2	67.2	130.5	101.4
5	5	57.4	172.8	84.0	163.2	126.8
6	6	68.9	207.3	100.7	195.8	152.1

It can be seen also in Figure 17 that the treatment of wind speed in ASHRAE HoF Wind model leads to unrealistically high estimations of air change rates.

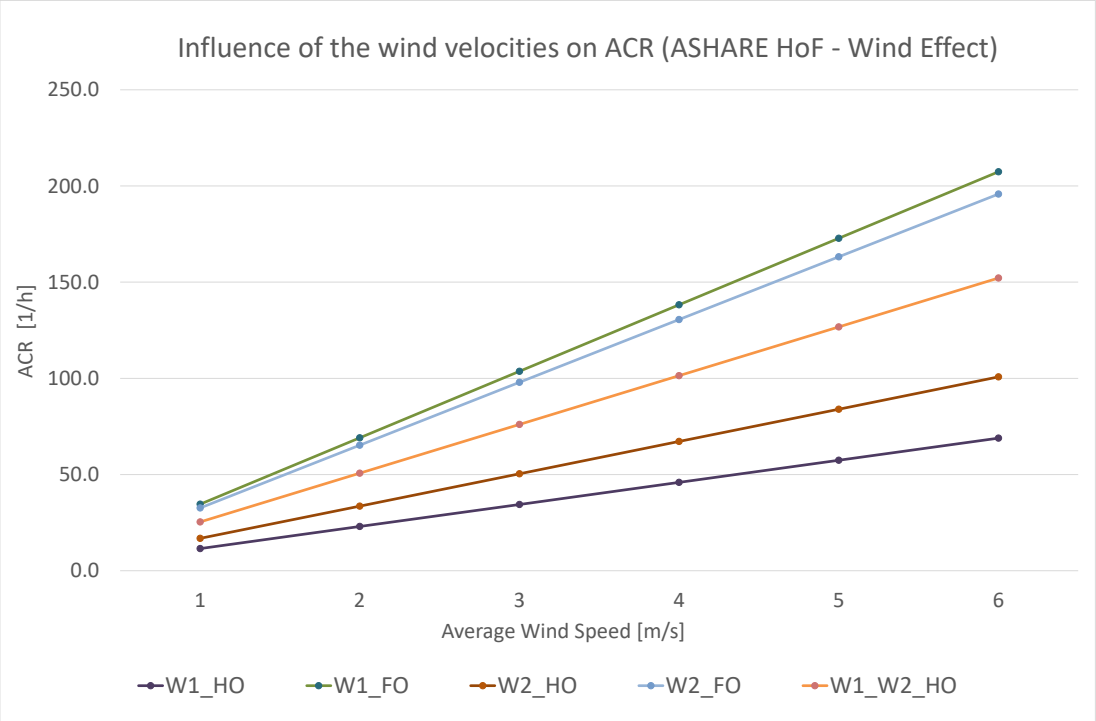

Figure 17 Influence of the wind velocities on air change rate in the case on ASHRAE HoF wind for the specific study cases

However, the calculation method for the ASHRAE HoF considering only the stack effect gives similar results to the other studied methods and close to the measurements as it can be seen in Table 9. Considering the uncertainties created by the influence of the wind effects it was decided to further analyze only the results given by the method for stack effect only.

Although it can be seen that the temperature difference between outside and inside air influences the results in the case of the method for the stack effect when comparing the same setups for window 1 and window 2 (half open and fully open), it seems that the size of the opening has also a significant influence in this method. For example, when comparing only the setups for window 1, namely half open and fully open, it can be observed that despite the temperature difference is almost 3 times higher in the case of window 1 half open, the case for fully open gives a higher air change rate as is being influenced by the size of the opening. Also, even though it was mentioned that case number 6 will not be further analyzed, here is presented just to show how the area of the opening influences the results when comparing case number 5 and case number 6. In the case of both windows fully open the air change rate is double as in the case of both windows half open, despite the similar temperature differences.

3.2.5 Warren's method

Table 12 presents the air change rates calculated with Warren's calculation method which proposes to calculate the effect of each driving force separately and then take the highest value from the two. During the time period when the measurements were made the wind had the predominant effect. This can also be noticed in the calculated air change rates as the maximum value of the two was always the value taking into consideration only the wind effect.

Table 12 Estimations of air change rate offered by Warren's calculation method

Measurement number	Window setup	Boundary conditions				ACR values [h^{-1}]	
		Ti,ave [K]	To,ave [K]	|ΔT| [K]	Average Wind Speed [m/s]	Measured	Warren
1	W1_HO	31.9	33.3	1.4	2.2	4.5	3.1
2	W1_FO	31.7	31.1	0.6	2.4	4.6	6.9
3	W2_HO	30.9	30.6	0.3	3.5	4.0	4.8
4	W2_FO	31.3	32.3	1.0	3.8	8.5	11.0
5	W1_W2_HO	32.3	36.5	4.2	4.7	21.9	13.0

3.3 Comparative analysis of the models' predictive performance

Table 13 presents the measured and the calculated air change rates for the eight different cases. Like previously mentioned in section 3.1, case number 6 is unclear due to the fact that the wind was predominantly blowing into the room during the measurements with high values of wind speeds which lead to high values of air change rates. Thus, it was decided to exclude case number 6 from further discussions and comparisons.

It can also be observed that the calculation methods offered from the ASHRAE's Handbook gave extreme values of air change rate. After addressing the uncertainties created by the influence of the wind direction in the sensitivity analysis made in section 3.2.4 it was decided to further analyze only the results given by the calculation method for stack effect only for the ASHRAE HoF method.

Table 13 Air change rates obtained through measurements and studied calculation methods

Measurement number	Window setup	Boundary conditions				ACR values [h^{-1}]					
		Ti,ave [K]	To,ave [K]	|ΔT| [K]	Average Wind Speed [m/s]	Measured	Hansen (VDI 2078)	De Gids & Phaff (EN 15242)	DS Method	ASHRAE HoF comb.	Warren
1	W1_HO	31.9	33.3	1.4	2.2	4.5	2.6	4.0	3.6	27.2	3.1
2	W1_FO	31.7	31.1	0.6	2.4	4.6	3.5	7.8	1.6	83.3	6.9
3	W2_HO	30.9	30.6	0.3	3.5	4.0	1.2	4.2	0.6	59.2	4.8
4	W2_FO	31.3	32.3	1.0	3.8	8.5	4.6	9.8	2.6	125.6	11.0
5	W1_W2_HO	32.3	36.5	4.2	4.7	21.9	9.0	12.5	9.2	124.4	13.0
6	W1_W2_FO	33.2	37.2	4.0	6.1	43.1	18.4	29.6	26.1	420.6	35.0
7	W1_T	32.6	35.4	2.8	4.7	3.1	1.1	2.1	-	-	-
8	W2_T	31.8	34.5	2.6	3.7	2.6	1.0	1.9	-	-	-

Another aspect addressed in this section is the measurement cases with tilted windows. As mentioned before and also showed in Table 13 only two of the studied methods offer separate equations for determining the effective area of the opening in case of tilted window: VDI 2078 Standard and the European Standard EN 15242:2007. Since the calculated air change rate for the case of tilted window with the equation for opening area proposed by EN 15242:2007 were closer to the measured air change rates (see Table 13) it was decided to use the respective window area in the other methods and see if similar results are obtained. However, as the DS Method does not consider the opening area as a parameter it was excluded from the respective calculation. An additional situation considered in the case of tilted window for the Hansen's method was to calculate the effective opening area as the sum of the three areas given by the window opening as shown in Figure 18. This specific case is referred in this work as "VDI_EA2".

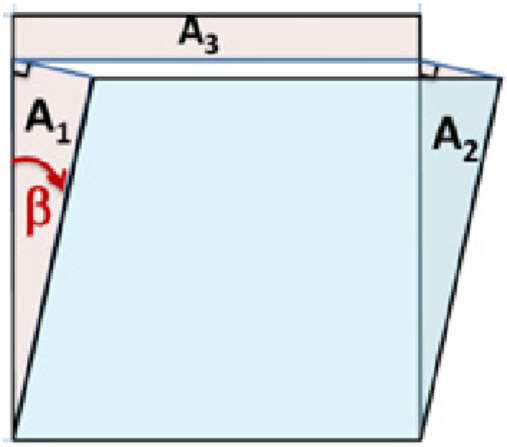

Figure 18 Areas considered in the calculation of the effective area for tilted windows for Hansen/ VDI 2078 method (source: Caciolo et al. 2011)

The calculation of the effective area was done by using the Equations 33, 34 and 35:

$$A_1 = A_2 = \frac{1}{2} * H * \sin\beta * \cos\beta \quad (33)$$

$$A_3 = L * H * (1 - \cos\beta) \quad (34)$$

$$A_{eff} = A_1 + A_2 + A_3 = H * (H * \sin\beta * \cos\beta + L - L * \cos\beta) \quad (35)$$

Considering that the dimensions of the window are 1.08 x 1.34 m with a tilt angle of 10º the resulting effective area for this specific case is 0.33 m^2.

The calculated air change rates in the case of tilted window can be seen in Table 14. So by using the opening area from the EN 15242, the calculation methods from EN15242, ASHRAE HoF stack and Warren gave similar results, while the one from VDI 2078 gave much lower air change rates. Also, it is observed that by using the effective area calculated with the Equation 35, the VDI_EA2 overestimates the air change rates and offers much higher estimations than the original VDI 2078 method and other methods. For that reason it was decided not to include the VDI_EA2 method in further discussions.

Table 14 Air change rates obtained through measurements and studied calculation methods in the case of tilted window

Measurement number	Window setup	Boundary conditions				ACR values [h^{-1}]					
		Ti,ave [K]	To,ave [K]	|ΔT| [K]	Average Wind Speed [m/s]	Measured	Hansen (VDI 2078)	VDI_EA2	De Gids & Phaff (EN 15242)	ASHRAE HoF stack	Warren
7	W1_T	32.6	35.4	2.8	4.7	3.1	1.1	4.6	2.1	2.0	2.3
8	W2_T	31.8	34.5	2.6	3.7	2.6	1.0	4.4	1.9	1.9	1.8

Another way to look at the results and to summarize the evidence for the present work was to disregard the models which have a lower performance or present uncertainties and average the rest. The disregarded models were the DS Method because it presented the worst performance when comparing to the other models for these study cases and the ASHRAE HoF for the wind effect because of its unrealistically high estimations of air change rates. This specific case is termed in this work as “MMP” meaning multi method prediction. The results of this method are shown in Table 15. A combination of the models takes into consideration the effect of both driving forces and could give results with good agreement to the measurements. In these studied cases it mainly underestimates the air change rates and gives a mean absolute

percentage error of 29 %. However, the number of measurements is too small to broaden this discussion and infer if such a method could offer reliable results.

Table 15 Estimated air change rates as the average of values obtained from four models

Measurement number	Window setup	ACR values [h^{-1}]						Relative error [%]
		Measured	Hansen (VDI 2078)	De Gids & Phaff (EN 15242)	ASHRAE HoF Stack	Warren	Average value of the 4 models (MMP)	
1	W1_HO	4.5	2.6	4.0	3.9	3.1	3.4	-24%
2	W1_FO	4.6	3.5	7.8	5.2	6.9	5.9	28%
3	W2_HO	4.0	1.2	4.2	1.8	4.8	3.0	-25%
4	W2_FO	8.5	4.6	9.8	6.8	11.0	8.0	-6%
5	W1_W2_HO	21.9	9.0	12.5	13.8	13.0	12.1	-45%
6	W1_T	3.1	1.1	2.1	2.0	2.3	1.9	-40%
7	W2_T	2.6	1.0	1.9	1.9	1.8	1.7	-37%
							Mean absolute percentage error	29%

Figure 19 shows the air change rates resulted from measurement in the different window setups and the ones calculated with the studied methods.

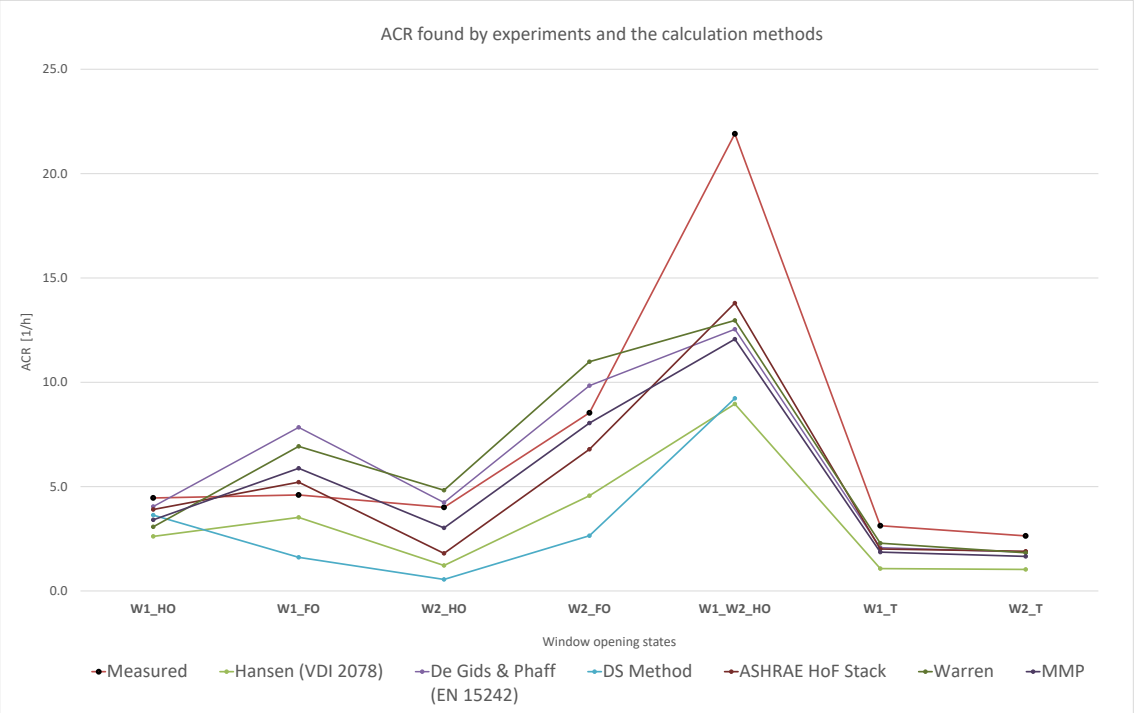

Figure 19 Air change rates found by experiments and studied calculation methods

Figure 20 compares the measured air change rates for the specific measurement cases with tracer gas with the calculated air change rates obtained from each studied

design model for natural ventilation. It can be seen how each model had performed in the specific cases. However, since there were just few measurements done a basis for a detailed discussion regarding the calculation methods performance is quite small.

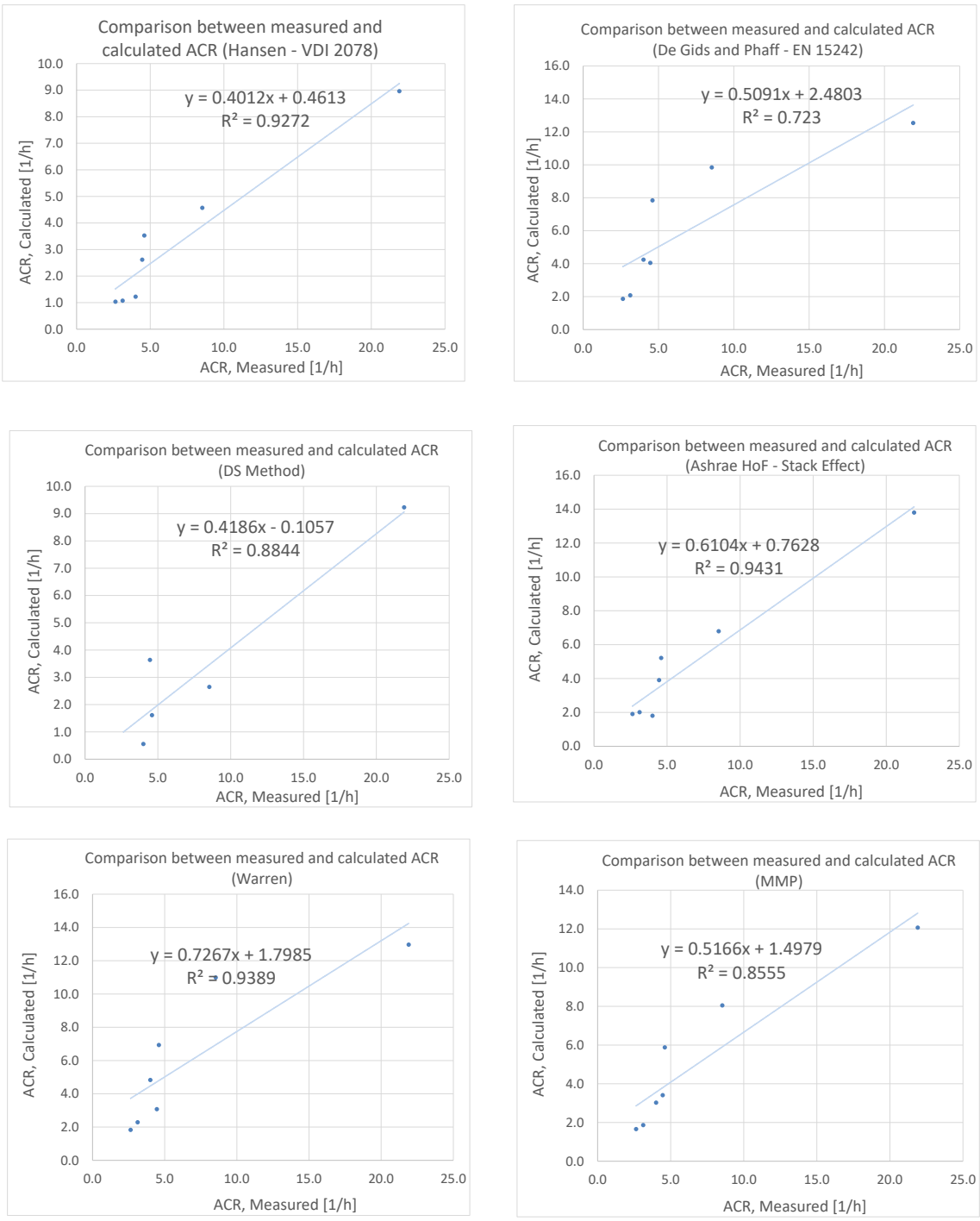

Figure 20 Comparison between measured and calculated air changes rates for the studied calculation methods

Table 16 summarizes the relative error calculated between the measured air change rates obtained through tracer gas measurements and the calculated air change rates from the five studied calculation methods. The idea is to see if the methods are under- or overestimating the air change rates. The relative error was calculated as shown in Equation 36:

*Relative error = (Calculated value –Measured value)/ Measured value * 100* (36)

In addition, the mean absolute percentage error is also calculated in order to obtain an overview of the predictions in these specific cases. This is presented as a total for all the investigated cases, but also by separating the case number 5 from the rest as this case with two half open windows presented a high air change rate during the measurements.

Table 16 Relative errors between the measured air change rates and the five studied calculation methods and the mean absolute percentage error

Measurement number	Window setup	ACR values [h^{-1}]							Relative error [%]					
		Measured	Hansen (VDI 2078)	De Gids & Phaff (EN 15242)	ASHRAE HoF Stack	Warren	DS Method	MMP	Hansen (VDI 2078)	De Gids & Phaff (EN 15242)	ASHRAE HoF Stack	Warren	DS Method	MMP
1	W1_HO	4.5	2.6	4.0	3.9	3.1	3.6	3.4	-41%	-9%	-12%	-31%	-18%	-24%
2	W1_FO	4.6	3.5	7.8	5.2	6.9	1.6	5.9	-23%	70%	13%	51%	-65%	28%
3	W2_HO	4.0	1.2	4.2	1.8	4.8	0.6	3.0	-70%	6%	-55%	20%	-86%	-25%
4	W2_FO	8.5	4.6	9.8	6.8	11.0	2.6	8.0	-46%	15%	-20%	29%	-69%	-6%
5	W1_W2_HO	21.9	9.0	12.5	13.8	13.0	9.2	12.1	-59%	-43%	-37%	-41%	-58%	-45%
6	W1_T	3.1	1.1	2.1	2.0	2.3	-	1.9	-66%	-34%	-36%	-27%	-	-40%
7	W2_T	2.6	1.0	1.9	1.9	1.8	-	1.7	-61%	-29%	-28%	-31%	-	-37%
		Mean absolute percentage error (all cases, except case 5)							51%	27%	27%	31%	60%	27%
		Mean absolute percentage error (all cases)							52%	29%	29%	33%	59%	29%

It can be seen in Figure 21 that the method developed by Hansen (VDI 2078) underestimates the air change rates in all the study cases. It needs to be mentioned that when the measurements were done the effect of the wind was more dominant than the temperature differences. The wind was blowing into the room which reduced the influence of the stack effect and since the method from VDI 2078 considers only stack effect, its performance was lower than the methods which consider the effect of the wind. However, the calculation method for the stack effect by ASHRAE HoF had a better performance than the one by VDI 2078 for this specific cases. The parameters of these models for the stack effect which might create this differences in results are the ones related to the window construction as they have different values for the effective opening area, the effective height of the window and the discharge coefficient C_D.

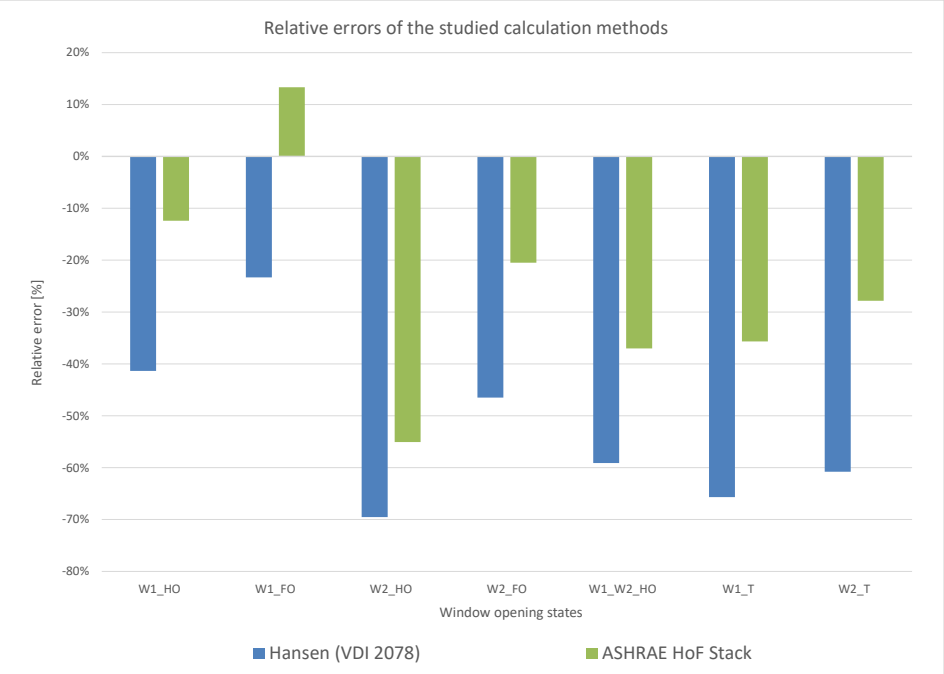

Figure 21 Relative errors for the Hansen's (VDI 2078) and ASHRAE HoF Stack method resulted for the investigated study cases

The models by De Gids and Phaff and by Warren which both consider the wind speed in their equations are mainly underestimating the air change rates (Figure 22). However, the results offered by De Gids and Phaff are slightly better for these measurement situations.

Figure 22 Relative errors for the De Gids & Phaff's (EN 15242) and Warren's method resulted for the investigated study cases

Also, as seen in Table 16, De Gids and Phaff and ASHARE HoF Stack methods have same values for the mean absolute percentage error. Yet, it can be seen that ASHRAE HoF Stack is mainly underestimating the results. One might argue that having a model that mainly underestimates is ok because the values are on the safe side when planning natural ventilation. On the other hand, considering that the wind had a dominant effect during the measurements, it makes sense to use models which includes the wind effect.

Figure 23 presents the mean absolute percentage error for all the calculation methods, including the MMP, resulted from the investigated study cases. It can be observed that the DS Method presented the worst performance from all the investigated methods in these study cases. This might be due the fact that this method only has the temperatures as influencing factors without considering the window construction or the wind effect. The multi method prediction (MMP) has the same mean absolute percentage error as the De Gids and Phaff and ASHRAE HoF Stack. However, the number of measurements is too small to infer if the multi method prediction could offer reliable results. It needs to be mentioned that this discussion is valid only for these specific study cases and weather conditions. Doing more measurements with different weather conditions could offer more information about the selected studied methods and broaden the discussion on their performance.

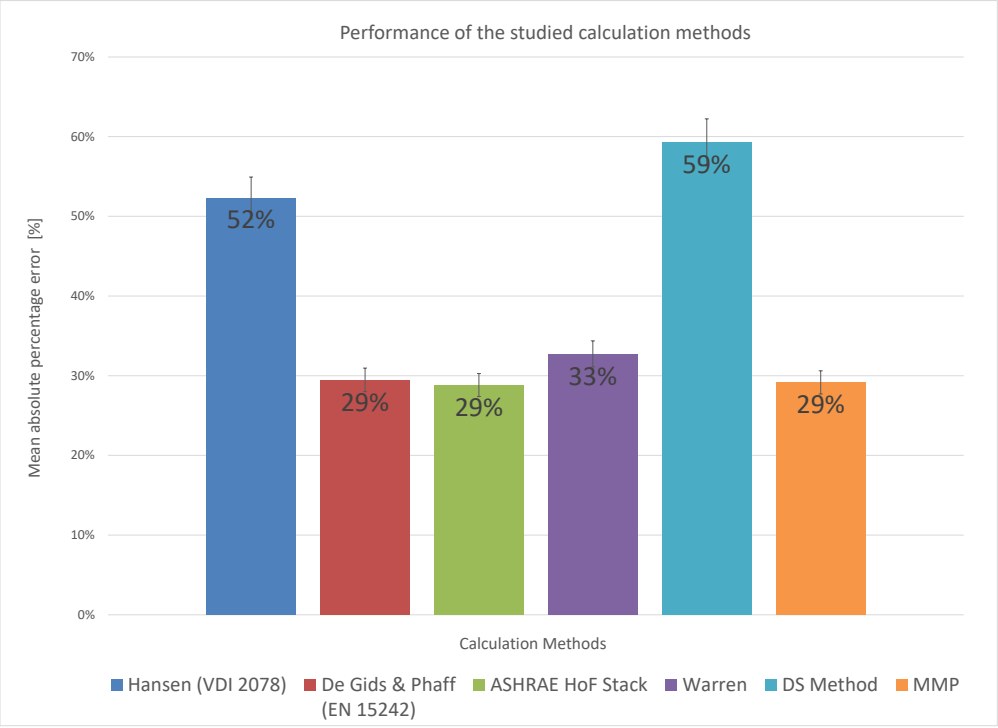

Figure 23 Performance of the studied calculation methods for the investigated study cases

4 CONCLUSION

An experimental study on single-sided ventilation has been presented in this thesis. The purpose was to evaluate five different single-sided natural ventilation calculation methods. Measurements have been made in a full-scale building exposed to outdoor conditions in Vienna, Austria. Although the number of measurements was too small to have a broad basis for conclusions, a few remarks could still be drawn from the results.

In the case of calculation methods considering only the thermal differences, the ASHRAE HoF give predicted values of air change rates closer to the measured one. Whereas in the case with a combination of the effects, the De Gids and Phaff (EN 15242) calculation method shows the best agreement with the experiments for these specific cases.

During the measurements it was observed that besides wind velocity and temperature difference, wind direction and opening area also have a significant effect on the air change rates. At that specific time when the measurements were done the wind was blowing into the test room which caused that the effect of the wind was higher than the stack effect. Moreover, the experimental results also show that the calculation methods react to these parameters. This can be seen in the poor performance of the models which consider only the stack effect, like the VDI 2078 or DS models. However, the ASHRAE HoF model considering only the stack effect had a better performance when compared to the other two models. The differences in these results offered by the calculation methods for the stack effect might be due to their parameters related to the window construction as they have different values for the effective opening area, the effective height of the window and the discharge coefficient C_D. Also, when discussing about the size of the opening area the predictions are mainly more accurate in the case of smaller openings. In the cases of tilted window the results are better when using the area proposed by EN 15242 as the one proposed by VDI 2078.

Taking into consideration the fact that the wind effect was dominant effect during the measurements, it makes sense to use models which includes the wind effect. The wind velocity is considered, together with the thermal differences, in the calculation method offered by De Gids and Phaff and by Warren. Although both are mainly overestimating the air change rates, the model by De Gids and Phaff offer slightly better results for these measurement situations. The ASHRAE HoF calculation method considering only the wind effect reacts very strongly to the wind direction

which leads to unrealistic estimation of air change rates. The model is also heavily dependent on its coefficient for the effectiveness of the opening given by the wind direction which resulted in unreliable values in these calculations. An adjustment of this coefficient could improve the model's accuracy. Nevertheless, considering that the measurements took place during the summer period, new measurements with higher temperatures differences and lower wind velocities are essential to broaden the discussion regarding the performance of these models.

Of course, the shape and surroundings of the building, layout of interior, geometry and position of the opening, turbulences in the wind and fluctuations in pressure at the opening also influence the air change rates, yet these aspects are out of the scope of simple calculation methods. However they are captured in detailed methods such as Computational Fluid Dynamics (CFD) or network models. Nevertheless, the current study provided empirical-based insights as to how to improve the simple estimation methods of air change rates toward enhancing the reliability of building performance analyses during the early design phase of a building.

5 INDEX

5.1 List of Figures

Figure 1 Natural ventilation principles: a) single-sided ventilation, b) cross ventilation and c) stack ventilation (source: Heiselberg 2006a) 4
Figure 2 Velocity profile of the airflow for a single-sided large opening in the case of ventilation driven by thermal buoyancy (source: Heiselberg 2006) 8
Figure 3 Diagram showing the dimensions of window frames and casements for tilted windows (source: VDI 2015) 11
Figure 4 Ratio of the flow through a bottom hung window and the fully open window (source: EN15242:2007) 13
Figure 5 a) The decay of the tracer gas concentration and b) Calculation of air change rate (source: “Building Monitoring and Diagnostics” lecture notes, TU Wien) 23
Figure 6 The test room at TU Wien (source: Google Maps) 24
Figure 7 Schematic plan of the test room (source: Department of Building Physics and Building Ecology, TU Wien) 25
Figure 8 Position of the two windows of the test room on the façade of TU Wien (Source: Google Maps) 25
Figure 9 WSBPI Weather station mounted on the roof of TU Wien (source: Pröglhöf 2009) 26
Figure 10 Temperature loggers mounted in the test room 27
Figure 11 Gas analyzer, SF_6 gas cylinder with pressure reducer and ventilator 27
Figure 12 Schematic plan of the test room with position of sensors 28
Figure 13 Screenshot of the excel tool created for the calculations of the studied calculation methods of single sided ventilation 29
Figure 14 Concentration decay for the measurement case “window 2 half open”; in linear scale (left), and in logarithmic scale (right) together with the linear regression and the air change rate as the decay coefficient 30
Figure 15 Concentration decay for the measurement case “window 2 fully open”; in linear scale (left), and in logarithmic scale (right) together with the linear regression and the air change rate as the decay coefficient 31
Figure 16 Concentration decay for the measurement case “window 2 tilted”; in linear scale (left), and in logarithmic scale (right) together with the linear regression and the air change rate as the decay coefficient 31
Figure 17 Influence of the wind velocities on air change rate in the case on ASHRAE HoF wind for the specific study cases 37

Figure 18 Areas considered in the calculation of the effective area for tilted windows for Hansen/ VDI 2078 method (source: Caciolo et al. 2011) 39
Figure 19 Air change rates found by experiments and studied calculation methods41
Figure 20 Comparison between measured and calculated air changes rates for the studied calculation methods.....42
Figure 21 Relative errors for the Hansen's (VDI 2078) and ASHRAE HoF Stack method resulted for the investigated study cases.....44
Figure 22 Relative errors for the De Gids & Phaff's (EN 15242) and Warren's method resulted for the investigated study cases 44
Figure 23 Performance of the studied calculation methods for the investigated study cases.....45

5.2 List of Tables

Table 1 Guidance for design stages for single-sided natural ventilation (source: Larsen et al. 2016)..... 7
Table 2 Selected existing calculation methods for the estimation of airflow rate in single-sided ventilation.....20
Table 3 Influencing parameters of the selected existing calculation methods.....22
Table 4 Window settings scenarios used in the measurements 22
Table 5 Measured boundary conditions and air change rates in the test room the air change rate.....32
Table 6 Estimations of air change rate offered by Hansen's (VDI 2078) calculation method 33
Table 7 Estimations of air change rate offered by De Gids & Phaff's (EN 15242) calculation method.....34
Table 8 Estimations of air change rate offered by the DS Method.....34
Table 9 Estimations of air change rate offered by ASHRAE HoF method 35
Table 10 Influence of the C_V coefficient on the air change rates for the specific measurement cases (ASHRAE HoF Wind) 36
Table 11 Influence of the wind velocity on the air change rates for ASHRAE HoF wind 36
Table 12 Estimations of air change rate offered by Warren's calculation method....38
Table 13 Air change rates obtained through measurements and studied calculation methods.....39
Table 14 Air change rates obtained through measurements and studied calculation methods in the case of tilted window.....40

Table 15 Estimated air change rates as the average of values obtained from four models.....41
Table 16 Relative errors between the measured air change rates and the five studied calculation methods and the mean absolute percentage error 43

5.3 List of Equations

(1) Calculation of volume flow rate caused by thermal buoyancy (Warren et al. 1985)……...…... 8

(2) Approximation Formulae for air exchange via windows due to the stack effect (VDI 2015)……..... 9

(3) Effective opening area in the case of fully open window, single window with inflow and outflow through the same window (VDI 2015)……. 9

(4) Effective opening height in the case of fully open window, single window with inflow and outflow through the same window (VDI 2015)……..10

(5) Effective opening area in the case of tilted window with a maximal tilt angle of 15°, single window with inflow and outflow through the same window (VDI 2015)……..10

(6) Effective opening height in the case of tilted window with a maximal tilt angle of 15°, single window with inflow and outflow through the same window (VDI 2015)……..10

(7) Height of the overlap between the window frame and casement in the case of tilted window with a maximal tilt angle of 15°, single window with inflow and outflow through the same window (VDI 2015)……..10

(8) The distance between the window frame and casement in the case of tilted window with a maximal tilt angle of 15°, single window with inflow and outflow through the same window (VDI 2015)…….10

(9) Calculation of tilt angle in the case of tilted window with a maximal tilt angle of 15°, single window with inflow and outflow through the same window (VDI 2015)……..11

(10) Correction factor for the window reveal in the case of tilted window with a maximal tilt angle of 15°, single window with inflow and outflow through the same window (VDI 2015)……..11

(11) Correction factor for the window reveal in the case of tilted window with a maximal tilt angle of 15°, single window with inflow and outflow through the same window (VDI 2015)……..11

(12) Air exchange via windows due to stack effect in the case of several windows at the same height in the room (VDI 2015)……....11

(13) Calculation of volume flow rate caused by wind, U_L (Warren et al. 1985)…..…..12

(14) Calculation of volume flow rate caused by wind, U_R (Warren et al. 1985)……..12

(15) Calculation of volume flow rate caused by thermal buoyancy and wind (Warren 1977)……..12

(16) Calculation of mean air velocity in the opening (EN 2007)……..……..12

(17) Calculation of air flow rate due to window opening (EN 2007)……..…..……..13

(18) Calculation of window opening area for the case of tilted window (EN 2007)…..13

(19) Calculation of air flow rate caused by thermal buoyancy and wind (Larsen 2006)……..14

(20) Calculation of the pressure differences in the opening (Larsen 2006)……..…..14

(21) Calculation of air flow caused by wind only (ASHRAE 2009)……..……14

(22) Calculation of air flow caused by thermal forces only (ASHRAE 2009)……..….14

(23) Calculation of air flow caused by wind and thermal forces (EnergyPlus 2015)..15

(24) Calculation of air flow caused by wind and thermal forces (Larsen et al. 2016)...15

(25) Calculation of air change rate caused by exterior temperature (Drees & Sommer ABT, 2015)……....16

(26) Calculation of air change rate caused by exterior temperature (Drees & Sommer ABT, 2015)……....16

(27) Calculation of air change rate caused by exterior temperature (Drees & Sommer ABT, 2015)……....16

(28) Calculation of air change rate caused by exterior temperature (Drees & Sommer ABT, 2015)……....16

(29) Calculation of air change rate caused by exterior temperature (Drees & Sommer ABT, 2015)……....16

(30) Calculation of air change rate caused by exterior temperature (Drees & Sommer ABT, 2015)……....16

(31) Calculation of air change rate caused by exterior temperature (Drees & Sommer ABT, 2015)……....16

(32) Calculation of gradient of straight line which gives the air change rate in the room (“Building Monitoring and Diagnostics” lecture notes, TU Wien, 2015)……23

(33) Calculation of effective opening area for the case of tilted window (Caciolo et al. 2011)…….40

(34) Calculation of effective opening area for the case of tilted window (Caciolo et al. 2011)…….40

(35) Calculation of effective opening area for the case of tilted window (Caciolo et al. 2011)…….40

(36) Calculation of relative error (Larsen et al. 2016)…….43

6 LITERATURE

ASHRAE (American Society of Heating Refrigerating and Air Conditioning Engineers), 2009. F16 SI : Ventilation and Infiltration.

ASTM International, 2011. Standard Test Method for Determining air Change in a Single Zone by Means of a Tracer Gas Dilution. *Standard, A.S.T.M., E741*.

Benedettelli, M. et al., 2015. Testing of a Tracer Gas Based Measurement Procedure to Assess Air Change Rates in Buildings. Available at: https://search.proquest.com/openview/bc7f2497ffa549e9eabb8515739f36c9/1?pq-origsite=gscholar&cbl=1646340.

Caciolo, M., Stabat, P. & Marchio, D., 2011. Full scale experimental study of single-sided ventilation : Analysis of stack and wind effects. *Energy & Buildings*, 43(7), pp.1765–1773. Available at: http://dx.doi.org/10.1016/j.enbuild.2011.03.019.

Cui, S. et al., 2015. CO2 tracer gas concentration decay method for measuring air change rate. *Building and Environment*, 84(November), pp.162–169.

Dick, J.B. and Thomas, D.A., 1951. Ventilation Research in Occupied Houses. *Journal of the Institution of Heating and Ventilating Engineers*, 19(194), pp.306–26.

EnergyPlus, 2015. Input Output Reference. *Bigladder Software*, (c), p.2109. Available at: http://bigladdersoftware.com/epx/docs/8-3/input-output-reference/index.html.

European Standards(EN), 2007. EN 15242-2007: Ventilation for buildings - calculation methods for the determination of air flow rates in buildings including infiltration.

Ghiabaklou, Z., 2010. Natural Ventilation as a Design Strategy for Energy Saving. , 4(11), pp.260–265.

De Gids, W. and Phaff, H., 1982. Ventilation rates and energy consumption due to open windows: a brief overview of research in the Netherlands. *Air infiltration review*, 4(1), pp.4–5.

Heiselberg, P.K., 2006a. Design of Natural and Hybrid Ventilation. , (Aalborg: Department of Civil Engineering, Aalborg University. (DCE Lecture Notes; No. 5).).

Heiselberg, P.K., 2006b. Modelling of Natural and Hybrid Ventilation. , (DCE(Aalborg: Department of Civil Engineering, Aalborg University. (DCE Lecture Notes; No. 4).).

Hellwig, R.T. et al., 2006. Thermal Comfort in Offices – Natural Ventilation vs . Air

Conditioning.

Howard-Reed, C., Wallace, L. a & Ott, W.R., 2002. The effect of opening windows on air change rates in two homes. *Journal of the Air & Waste Management Association (1995)*, 52(2), pp.147–159.

International Organization for Standardization (ISO), 2012. ISO 12569: Thermal Performance of Buildings and Materials—Determination of Specific Airflow Rate in Buildings—Tracer Gas Dilution Method.

Iwashita, G. and Akasaka, H., 1997. The effects of human behavior on natural ventilation rate and indoor air environment in summer—a field study in southern Japan. *Energy and Buildings*, 25(3), pp.195–205.

Kvisgaard, B. and Collet, P.F., 1990. The user's influence on air change. *Air change rate and airtightness in buildings*, pp.67–76.

Larsen, T.S., 2006. *Natural Ventilation Driven by Wind and Temperature Difference*. Phd dissertation: Aalborg University.

Larsen, T.S. & Heiselberg, P., 2008. Natural ventilation driven by wind pressure and temperature difference. , 40(2), pp.1031–1040.

Larsen, T.S., Plesner, C. & Leprince, V., 2016. Calculation methods for single-sided natural ventilation - simplified or detailed? *Proceedings of Clima 2016*, (May), p.10.

Laussmann, D. & Helm, D., 2011a. Air Change Measurements Using Tracer Gases. *Chemistry, Emission Control, Radioactive Pollution and Indoor Air Quality*, pp.365–404.

Persily, A.K., 1997. Evaluating building IAQ and ventilation with indoor carbon dioxide. *ASHRAE Transactions*, 103(pt 2), pp.193–204.

Persily, A.K., 1996. The relationship between indoor air qualiti and carbon dioxide.pdf. *Indoor Air '96: The 7th International Conference on Indoor Air Quality and Climate*, pp.961–966.

Plesner, C., Larsen, T.S. & Leprince, V., 2015. Evaluation of single-sided natural ventilation using a simplified and fair calculation method. , (July).

Pröglhöf, C.; A.M., 2009. *On patterns of control-oriented human behavior in office environments*. Phd dissertation: Technischen Universität Wien.

Raatschen, W., 1995. Tracergasmessungen in der Gebäudetechnik. , 116.

Roulet, C. and Scartezzini, J.L., 1987. Measurement of air change rate in an inhabited building with a constant tracer gas concentration technique. *ASHRAE*

Transactions, 93, pp.1371–1380.

Seppänen, O.A. and Fisk, W.J., 2004. Summary of human responses to ventilation. *Indoor Air*, 14(7), pp.102–118.

Seppänen, O. a, Fisk, W.J. & Mendell, M.J., 1999. Association of ventilation rates and CO2 concentrations with health and other responses in commercial and institutional buildings. *Indoor air*, 9(4), pp.226–252.

Sherman, M.H., 1990. Tracer-gas techniques for measuring ventilation in a single zone. *Building and Environment*, 25(4), pp.365–374.

Traynor, G.W., Apte, M.G., Carruthers, A.R., Dillworth, J.F., Prill, R.J., Grimsrud, D.T. and Turk, B.H., 1988. The effects of infiltration and insulation on the source strengths and indoor air pollution from combustion space heating appliances. *JAPCA*, 38(8), pp.1011–1015.

Verein Deutscher Ingenieure-Fachbereich Technische Gebäudeausrüstung, 2015. VDI 2078 Calculation of thermal loads and room temperatures (design cooling load and annual simulation.

Verein Deutscher Ingenieure-Fachbereich Umweltmesstechnik, 2001. VDI 4300 Bestimmung der Luftwechselzahl in Innenräumen air change rate.

Wargocki, P., Sundell, J., Bischof, W., Brundrett, G., Fanger, P.O., Gyntelberg, F., Hanssen, S.O., Harrison, P., Pickering, A., Seppänen, O. and Wouters, P., 2002. Ventilation and health in non-industrial indoor environments: report from a European Multidisciplinary Scientific Consensus Meeting (EUROVEN). *Indoor Air*, 12(2), pp.113–128.

Warren, P., 1977. Ventilation through openings on one wall only, Energy conservation in heating, cooling, and ventilating buildings. In *Int. Conf. Heat and Mass Transfer in Buildings*. pp. 189–209.

Warren, P.R. & Parkins, L.M., 1985. Single-Sided ventilation through open windows. In *Proceedings, Thermal performance of the exterior envelopes of buildings, Florida, ASHRAE SP 49*. pp. 209–228.

Wilson, A.L., Colome, S.D., Tian, Y., Becker, E.W., Baker, P.E., Behrens, D.W., Billick, I.H. and Garrison, C.A., 1996. California residential air exchange rates and residence volumes. *Journal of Exposure Analysis and Environmental Epidemiology*, 6(3), pp.311–326.

Yamanaka, T., Kotani, H., Iwamoto, K. and Kato, M., 2006. Natural, wind-forced ventilation caused by turbulence in a room with a single opening. *International Journal of Ventilation*, 5(1), pp.179–187.

Yan, Y. et al., 2007. Measuring air exchanges rates using continuous CO2 sensors. *Air and Waste Management Association - Symposium on Air Quality Measurement Methods and Technology 2007*, 165 CP, pp.101–108. Available at: https://www.scopus.com/inward/record.uri?eid=2-s2.0-52049103863&partnerID=40&md5=d7b129163cc9b661d356aa17e65395c4.

Zhai, Z. (John), Mankibi, M. El & Zoubir, A., 2015. Review of Natural Ventilation Models. *Energy Procedia*, 78(0), pp.2700–2705. Available at: http://linkinghub.elsevier.com/retrieve/pii/S1876610215020871.

7 APPENDIX

A. Technical specification of WSBPI (Thies 2007)

Sensor / Device name or number	Range	Accuracy
Temperature/Relative humidity: "Hygro-Thermogeber compact 1.1005.54.161"	Temp: -30°C to +70°C RH: 0 to 100%	Temp: +0.2 K at 20°C and wind speed >1.0 $m \cdot s^{-1}$ RH: ±2%
Solar radiation: „Pyranometer CM3 by Kipp & Zonen 7.1415.03.000"	0 to 1400 $W \cdot m^{-2}$	Sensitivity ±0.5% Applied correction +2%
Illuminance: "V-Lambda Strahlungssensor 4.3"	0 to 130 klx	
Wind speed: "Windgeber compact 4.3519.00.000 beheizt"	0.5 to 50 $m \cdot s^{-1}$	Accuracy ± 3% or ± 0.5 $m \cdot s^{-1}$ Resolution <0.1 $m \cdot s^{-1}$
Wind direction: "Windrichtungsgeber compact 4.3129.00.000"	0 to 360°	Accuracy ± 5 ° Resolution 11.25°
Precipitation: "Niederschlagsgeber 5.4032.30.007 ohne Heizung"	max 7 $mm \cdot Min^{-1}$ 0°C to +60°C	0.1 mm Precipitation
Barometer: "Barogeber PTB100A 3.1158.00.073"	800 to 1600 hPa	+20°C - ±0.3 hPa 0°C to 40°C - ±1 hPa -20°C to +45°C - ±1.5 hPa -40°C to +60°C - ±2.5 hPa
Data logger: "MeteoLOG TDL 14"	Operating Range: -30°C to +50°C	±0.2% of measurement range Time Accuracy: not decisive

B. Technical specifications Innova Gasmonitor 1312

Product Data

1312 Photoacoustic Multi-gas Monitor

USES:

- Quantitative analysis of up to 5 components and water vapour in gas mixtures
- Occupational health and safety measurements
- Indoor air-quality and ventilation measurements
- Detection of accidental releases of gases/vapours
- Presentation of measurement data in spreadsheet, database and word processing programs

FEATURES:

- Selectively measures a wide range of gases/vapours
- Linear response over a wide dynamic range
- Extremely reliable due to self-testing procedures
- High stability (low drift) makes calibration only necessary about four times a year
- User-friendly procedures for calibrating the monitor, presenting and analysing measurement data via the PC user-interface
- Accurate — compensates for temperature fluctuations, water-vapour interference and interference from other known gases
- Seven *Sample Integration Times* to choose from — to optimize the measurement system, providing faster response times or lower detection limits
- Extremely low-volume flushing possible
- Operates immediately — no warm-up time necessary
- Collects samples from points up to 50 m away
- Presents measurement data both in tabular and graphic formats – up to 6 gas concentration graphs displayed, simultaneously
- Uses Open Database Connectivity (ODBC) — enabling measurement data to be used in other programs
- Portable
- Operates also as stand-alone instrument
- Monitor can be used with one/two 1303 Multipoint Doser and Sampler units + additional PC software for ventilation efficiency measurements

Introduction

The 1312 Photoacoustic Multi-gas Monitor is a highly accurate, reliable and stable quantitative gas monitoring system. Its measurement principle is based on the photoacoustic infrared detection method. This means that the 1312 can measure almost any gas which absorbs infra-red light. Appropriate optical filters (up to 5) are installed in the 1312's filter carousel so that it can selectively measure the concentration of up to 5 component gases and water vapour in any air sample. The 1312's detection limit is gas-dependent, but typically in the ppb region.

Reliability of measurement results can be ensured by regular self-tests which the 1312 performs. Accuracy is ensured by the 1312's ability to compensate any measurement for temperature fluctuations, water-vapour interference and interference from other gases known to be present.

The monitoring system is easily operated via a PC, or via the front-panel push-buttons when using a stand-alone instrument configuration. Short explanatory text guide the user through each operating procedure. Therefore, no special training is required to operate the 1312.

The 1312PC software enables the user to calibrate the monitor and load the user-defined measurement setups prior to monitoring. During a monitoring task, real-time measurement data is presented on screen as both graphs and tables, and the data is stored in named databases. When a monitoring task is completed, the 1312PC software can assist in analysing the data. The measurement data stored in the databases is easily accessible, and can be displayed on screen, printed out, and

INNOVA
AirTech Instruments

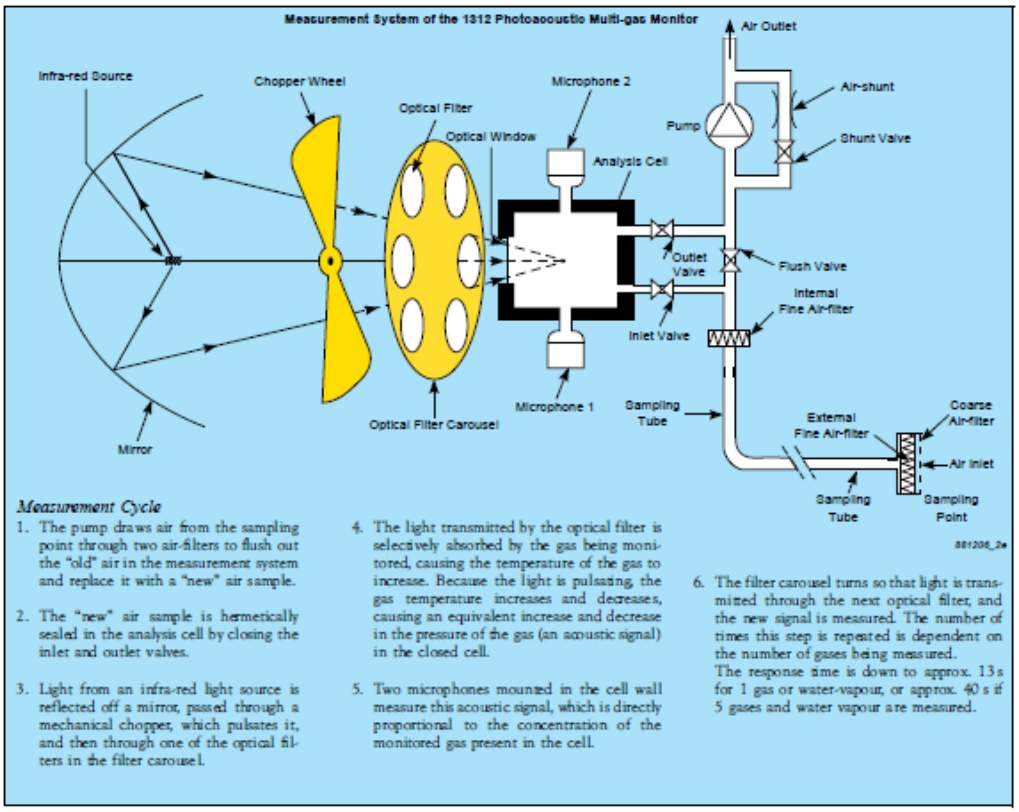

Measurement Cycle

1. The pump draws air from the sampling point through two air-filters to flush out the "old" air in the measurement system and replace it with a "new" air sample.
2. The "new" air sample is hermetically sealed in the analysis cell by closing the inlet and outlet valves.
3. Light from an infra-red light source is reflected off a mirror, passed through a mechanical chopper, which pulsates it, and then through one of the optical filters in the filter carousel.
4. The light transmitted by the optical filter is selectively absorbed by the gas being monitored, causing the temperature of the gas to increase. Because the light is pulsating, the gas temperature increases and decreases, causing an equivalent increase and decrease in the pressure of the gas (an acoustic signal) in the closed cell.
5. Two microphones mounted in the cell wall measure this acoustic signal, which is directly proportional to the concentration of the monitored gas present in the cell.
6. The filter carousel turns so that light is transmitted through the next optical filter, and the new signal is measured. The number of times this step is repeated is dependent on the number of gases being measured. The response time is down to approx. 13 s for 1 gas or water-vapour, or approx. 40 s if 5 gases and water vapour are measured.

exported to other spreadsheet, database and word processor programs when required.

If a stand-alone configuration is required, the monitor can be operated using the front panel push-keys. The measurement results are stored in the monitor's memory, and can be uploaded to the PC or printed at a later stage.

The 1312 has a sturdy, dust-proof casing to protect its components. It is portable, and requires no warm-up time or re-calibration after moving — making it ideal for short-term monitoring of air samples drawn from its immediate environment. For long-term monitoring, the 1312 is placed indoors and collects air samples for analysis, via tubing, from points up to 50 m away.

Selectivity

The selectivity of the 1312 is determined by the optical filters installed in it's filter carousel. A wide range of narrow-band optical filters is available from Innova AirTech Instruments. By studying the absorption spectra of the gases to be monitored, as well as those of any other gases which may be found in the ambient air in the same area, the most appropriate optical filters can be chosen. Please refer to the Gas Detection Limits chart for details.

Water vapour, which is nearly always present in ambient air, absorbs infra-red light at most wavelengths so that, irrespective of which optical filter is used, water vapour will contribute to the total acoustic signal in the analysis cell. The higher the concentration of water vapour in the cell, the more it contributes to the measured signal. However, a special optical filter is permanently installed in the filter carousel of the 1312, which allows water-vapour's contribution to be measured separately during each measurement cycle. The 1312 is thus able to compensate for water-vapour's interference.

Any other interferent gas, which is known to be present in the ambient air, can be compensated for in a similar fashion. By installing an optical filter to selectively measure the concentration of the interferent gas, the user can set-up the 1312 to compensate for the interferent gas's contribution.

Calibration

After the relevant optical filters are installed, the monitor must be calibrated. Four types of calibration are available: zero-point, humidity-interference, humidity-span and gas calibration. Regardless of the calibration type, the 1312PC software makes it easy. Setting up the calibration is done via the familiar Windows®95 environment. The raw measurement data from the monitor is transferred to the PC where it is displayed graphically. Using the cursors in the graphic window, the best ranges can be defined. The raw data in these areas is used to produce the offset calculation values to enable humidity interference and cross-compensation. Only when you are satisfied with the result, are these calculation values downloaded to the monitor.

Due to the 1312's high stability (low drift), calibration is seldom necessary more than four times a year.

Operation

The 1312 monitoring system is easy to operate, either directly via a PC or via the push-keys on the monitor's front panel. This enables the monitor to be operated as both an on-line and stand-alone instrument.

You define all the information necessary to start a monitoring task. The PC uses menu bars and "index-card" labelled windows to divide the procedures in to logical sections. The front panel push-buttons are supported by short explanatory texts, guiding the operator through the procedures.

Setting-up the Monitor

Each monitoring task is given a distinct name. Under this name, the setup option enables you to define all the parameters necessary for the monitoring task to be completed. The *Sample Integration Times* (S.I.T.) are defined here (see Fig.2). This allows you to decide the measurement accuracy against the speed of the measurements. The monitor can be set to measure at one of seven different S.I.T.s (from 0.5 s to 50 s). The shortest S.I.T.s enable many measurements to be made quickly where the accuracy of the results are not crucial, while the longest S.I.T.s enable highly accurate results to be obtained. A separate S.I.T. can be selected for each filter.

This setup option also enables you to select if cross-compensation for known interferents and water vapour should occur, as well as decide on the sampling mode (continuous or fixed time interval). The flushing time is also set here. You decide whether only the measurement chamber is flushed, using a minimal gas sample, or whether the chamber and sampling tubing should be flushed and the length of time this should take. Alternatively, the monitor can be set to find the optimal flushing time, automatically.

Should some form of warning be necessary, the software enables the user to set minimum and maximum alarm trigger levels for each measured gas. It is also possible to define what action is taken when an alarm is triggered.

Starting Measurements

Once the setup parameters have been defined, measurements can be started immediately. Alternatively, a delayed start time can be defined. The PC and the monitor have synchronized clocks, so whether the monitor is operating on-line or stand-alone, the measurements will start at the correct time. The monitoring task will continue until it is stopped manually, or a stop time can be defined, enabling the system to run completely unattended.

Memory Mode

This option is available when the monitor is operating as a stand-alone instrument. During a monitoring task, all results are stored in a memory called *Display Memory*. While operating in Memory mode, data in this memory can be copied into the 1312's other memory (*Background Memory*) to prevent it being overwritten by results from the next task.

Data stored in *Background Memory* can be recalled to *Display Memory* and then can be uploaded to a PC.

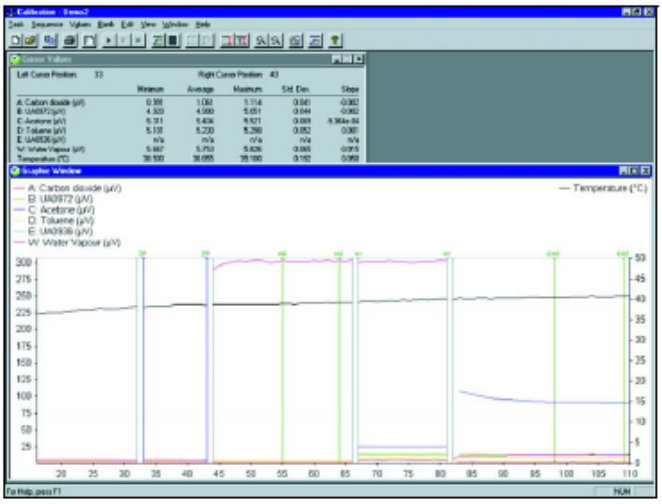

Fig.1 Calibration curves, including their cursors showing the regions used to calculate the calibration factors, which can be downloaded to the monitor

Alarms

When on-line measurements are being made, the software enables the user to set trigger, minimum, and maximum alarm levels for each measured gas. It is also possible to define what action is taken when an alarm is triggered.

Measurement Results

On-line Measurements

Measurement results are transferred directly to the PC. Here they can be displayed on screen as real-time values in tables and graphs. The graphs can be set up to display only the desired gases, within defined concentration ranges and results from statistical analyses.

Regardless of what is displayed on screen, all measurement data is stored in user-defined databases, in an MS-Access® format. This makes results readily available to view at a later stage for further analyses, or for inclusion in other programs, for example, Excel™ or Word®. The 1312PC software, with its Open Database Connectivity (ODBC), enables result data to be utilized by any programs using this form of data exchange.

Stand-alone Measurements

Gas-measurement results are displayed on the 1312's screen as soon as they are available, and are constantly updated. During a task, the 1312 performs a running statistical analysis of measured gas concentrations, calculating for each monitored gas: the Mean Value; the Standard Deviation; and the Maximum and Minimum measured concentrations. The Mean Value is the same as the Time-Weighted Average (TWA) value during the total monitoring period.

The individual results stored in *Display Memory* can also be automatically averaged and presented on the display.

Measurement data stored in the 1312's *Display Memory* can be printed out in list form on any standard text-printer, via the IEEE 488 or RS-232 interfaces.

If any interesting or unusual event occurs during a monitoring task, the measurement being performed at this time can be "marked". This enables the user to assess the event's affect on the monitoring task.

When the monitor is once again connected to a PC, all the measurement results can be uploaded. These can then be viewed and used similar to the on-line gas measurement results.

Exporting Data

If measurement results need to be used by other instruments in the process, or by programs which can not use ODBC, data can be exported as semicolon delimited ASCII files.

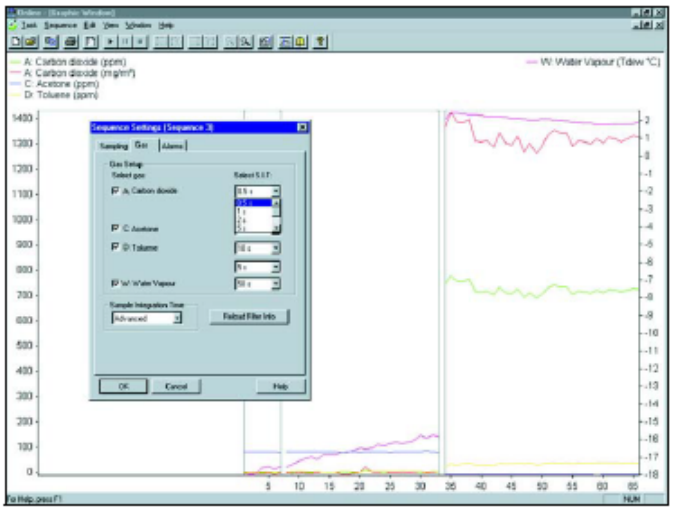

Fig. 2 Setting up the Sample Integration Times for the individual filters.

Reliability

Reliability can be ensured by a series of self-tests which the monitor can perform. The self-tests, which can be disabled if required, check software, data integrity, and the components of the 1312 to ensure that they function properly. If any fault is found, it is reported in the measurement results so that users can see what, if anything, has affected the accuracy of the measurement.

If there is an AC mains power-supply failure, the 1312 will automatically start-up again when power is restored. Measurement data is stored in the monitor's memory and can be uploaded to the PC when the software has been restarted.

Maintenance

The only maintenance tasks necessary are calibration and changing the filters in the internal and external air-filtration units of the 1312. Both tasks are easily performed, and are typically necessary only four times a year.

Other Remote Control Options

Innova AirTech Instruments also offers two additional application software programs, the 7300 Application Software and the 7620 Application Software.

Using the 7300, a computer can remotely control a 1312 together with one 1309 Multipoint Sampler for sequentially monitoring air-samples from up to 12 locations.

Using the 7620, a computer can control a 1312 together with up to two 1303 Multipoint Sampler and Doser Units. This enables up to 12 locations to be dosed with a tracer-gas and air-samples to be drawn from each location for analysis by the 1312. The software uses the resultant measurements to calculate the air-change or ventilation efficiency of each location.

Specifications 1312

WARNING! *The 1312 must not be placed in areas with flammable gases/vapours in explosive concentrations, or be used to monitor explosive concentrations of these. Also, monitoring of certain aggressive gases, or a very high concentration of water vapour, could damage the 1312. Ask your local Innova representative for further information.*

All terms relating to gas analysis are in accordance with the definitions set out in the ISO International Standard 8158.
Your local Innova representative will assist in the selection of suitable optical filters. Details are provided in the "Optical Filters" Product Data Sheet and the Gas Detection Limits wall-chart.

MEASUREMENT TECHNIQUE:
Photoacoustic infra-red spectroscopy.

RESPONSE TIME:
(including chamber flushing) is dependent on the sample integration time (S.I.T.) and the flushing time defined. The fastest response time for one gas is 13 s and for 5 gases and water vapour 40 s, but see the examples below:

Monitor Setup	Response Times
S.I.T.: "Normal" (5s) Flushing: Auto, (Tube 1m)	One gas: ~25s 5 gases + water: ~75s
S.I.T.: "Fast" (1s) Flushing: Tube "OFF" Chamber 4s	One gas: ~15s 5 gases + water: ~45s

MEASUREMENT RANGE:♠
Detection Limit: gas-dependent, but using the "Gas Detection Limits" wall-chart, the limits can be calculated using the following multiplication factors:

S.I.T.	0.5	1	2	5	10	20	50
Factor	3	2.2	1.6	1	0.7	0.5	0.3

Note: an individual S.I.T. can be selected for each filter

Dynamic Range: five orders of magnitude (i.e. upper limit = 100 000 times the detection limit). To measure over this wide dynamic range, span-calibration must be performed with two different gas concentrations.

MEASUREMENT UNITS: (1312PC)
mg/m^3, g/m^3, μ/m^3
ppm, vol%, ppb

ACCURACY:
Zero Drift: Typically ±Detection limit♠ per 3 months●.
Influence of temperature♦: ±10% of detection limit♠/°C.
Influence of pressure ♥: ±0.5% of detection limit♠/mbar.
A concentration of 100 × detection limit♠ was used in determining these specifications:
Repeatability: 1% of measured value●
Range Drift: ±2.5% of measured value per 3 months●.
Influence of temperature♦: ±0.3% of measured value/°C.
Influence of pressure♥: – 0.01% of measured value/mbar.
Reference conditions:
● Measured at 20°C, 1013 mbar, and relative humidity (RH): 60%.
♦ Measured at 1013 mbar, and RH: 60%.
♥ Measured at 20°C and RH: 60%.

♠ Measured detection limit is @5s S.I.T.
INTERFERENCE:
The 1312 automatically compensates for temperature fluctuations in its analysis cell, and can compensate for water vapour in the air sample. If an optical filter is installed to measure a known interferent, the 1312 can cross-compensate for the interferent.
DATA STORAGE CAPACITY: (for stand-alone)
Dependent on the number of gases being measured. Sufficient for a 12-day monitoring task, monitoring 5 gases and water vapour every 10 min.
GENERAL:
Dimensions:
Height: 175 mm (6.9 in).
Width: 395 mm (15.6 in).
Depth: 300 mm (11.8 in).
Weight: 9 kg (19.8 lbs).
Maximum Pumping Rate: 30 cm^3/s (flushing sampling tube) and 5 cm^3/s (flushing measurement chamber).
Minimum Volume of Air required per sample:
Power Requirement: 100–127V and 200–240V (50 – 400 Hz) ±10% AC. Complies with IEC536 Class 1 Safety Standards.
Power Consumption: ~100 VA.

Flushing Settings	Volume of Air
Auto: Tube Length: 1m	140 cm^3/sample
Fixed Time: Chamber 2s, Tube 3s	100 cm^3/sample
Fixed Time: Chamber 2s, Tube "OFF"	10 cm^3/sample

Alarm Relay Socket: for connection to one or two alarm relays (visual/audio). Alarm levels for each gas are user-defined.
Acoustic Sensitivity: not influenced by external sound.
Vibration Sensitivity: complies with IEC 682-6. Strong vibrations at 20 Hz can affect the detection limit.
Back-up Battery: 3V lithium battery, life-time 5 years. This protects data stored in memory, and powers the internal clock.

COMMUNICATION:
The monitor has an IEEE488 and an RS-232 interface, for data exchange and remote control of the 1312. The 1312PC communicates using the RS-232.

1312PC SOFTWARE
Supplied on 3.5 inch disks.
Computer Requirements:
Hardware:
A 486 (50MHz) processor or better.
Min. 16Mbytes of RAM.
Min. 40Mbytes of space available on the hard disk.
VGA monitor or better.
One RS–232 port.
Mouse.

Software:
Windows®95.

COMPLIANCE WITH STANDARDS:

CE	CE-mark indicates compliance with: EMC Directive and Low Voltage Directive.
Safety	EN 61010–1 (1993) & IEC 1010–1 (1990): Safety requirements for electrical equipment for measurement, control and laboratory use.
EMC Emission	EN 50081–1 (1992): Generic emission standard. Part 1: Residential, commercial and light industry. EN 50081–2 (1993): Generic emission standard. Part 2: Industrial environment. CISPR 22 (1993): Limits and methods of radio disturbance characteristics of information technology equipment. Class B Limits. FCC Class B limits.
EMC Immunity	EN 50082–1 (1992): Generic immunity standard. Part 1: Residential, commercial and light industry. RF immunity implies that gas concentration indications greater than 150 times the detection limit will be affected by no more than ± 5% @5s S.I.T. EN 50082–2 (1995): Generic immunity standard. Part 2: Industrial environment. RF immunity implies that gas concentration indications greater than 500 times the detection limit will be affected by no more than ± 5% @5s S.I.T. Note: The above is guaranteed using accessories listed in this Product Data sheet only.
Temperature	IEC68–2–1 & IEC68–2–2: Environmental Testing. Cold and Dry Heat. Operating Temperature: +5°C to +40°C (+41°F to +104°F). Storage Temperature: –25 to +55 °C (–13°F to +131°F).
Humidity	IEC68–2–3: 90% RH (non-condensing at 30°C).
Enclosure	IEC529: IP 20.
Mechanical	IEC68–2–6: Vibration: 0.3 mm, 20 m/s^2, 10–500 Hz. IEC68–2–27: Shock: 1000 m/s^2. IEC68–2–29: Bump: 3000 bumps at 250 m/s^2.